J. Paleont., 80(1), 2006, pp. 49–71

0022-3360/06/0080-49$03.00

MORPHOLOGICAL DIFFERENTIATION OF AVICULARIA AND THE PROLIFERATION OF SPECIES IN MID-CRETACEOUS *WILBERTOPORA* CHEETHAM, 1954 (BRYOZOA: CHEILOSTOMATA)

ALAN H. CHEETHAM,[1] JOANN SANNER,[1] PAUL D. TAYLOR,[2] AND ANDREW N. OSTROVSKY[3]

[1]Department of Paleobiology, National Museum of Natural History, Smithsonian Institution, Washington, DC 20650, <cheetham@si.edu, sannerj@si.edu>, [2]Department of Palaeontology, The Natural History Museum, London SW7 5BD, England, <pdt@nhm.ac.uk>, and [3]Department of Invertebrate Zoology, Faculty of Biology and Soil Science, St. Petersburg State University, Universitetskaja nab. 7/9, 199034 St. Petersburg, Russia <oan_univer@yahoo.com>

ABSTRACT—Discovery of avicularium-like polymorphs in *Wilbertopora mutabilis* Cheetham, 1954 has provided not only a new opportunity for revising the genus *Wilbertopora* Cheetham, 1954, but also a more detailed basis for documenting the series of morphological changes by which avicularia differentiated from ordinary feeding zooids in what appears to be the first occurrence of these characteristic cheilostome bryozoan structures in the fossil record.

Eighteen of a total 60 quantitative characters measured on avicularia and ordinary and ovicell-bearing autozooids were sufficient to distinguish eight species of *Wilbertopora* by discriminant function analysis of zooid data from 93 colonies from the mid-Cretaceous (Albian–Cenomanian) Washita Group in northeastern Texas and southeastern Oklahoma. Eighteen of a total of 20 of the quantitative characters that could be statistically coded for cladistic analysis proved to be informative with respect to parsimony, providing two maximally parsimonious trees for the eight species. Two-thirds of the diagnostic characters involve avicularia. An additional 55 colonies too poorly preserved for morphometric analysis could then be assigned to species qualitatively, with 170 more colonies lacking species-diagnostic characters.

The cladistic trees strongly suggest that most or all of the species diverged before the end of the Albian, but stratigraphic resolution is insufficient to test this hypothesis. Nevertheless, the series of morphological changes differentiating avicularia from ordinary autozooids in these species, based on the cladistic relationships, is highly significant statistically, and may be a pattern later repeated in other cheilostomes.

Wilbertopora and *W. mutabilis* are emended, and seven new species are described: *W. listokinae*, *W. tappanae*, *W. spatulifera*, *W. attenuata*, *W. improcera*, *W. acuminata*, and *W. hoadleyae*.

INTRODUCTION

THE GENUS *Wilbertopora* Cheetham, 1954 occupies a significant place in the early radiation of the Cheilostomata, which appeared first in Late Jurassic time (Taylor, 1994) and subsequently proliferated rapidly to become the dominant order of Bryozoa in modern seas. Morphological features that characterize a broad spectrum of cheilostome taxa—such as multiserial colony growth, in which zooids communicate not only with those from which they budded but also with those in adjacent budding rows; calcified chambers (ovicells) in which embryos are brooded; and avicularia, zooids with opercula and associated musculature modified to perform such functions as defense, cleaning, and in some modern cheilostomes even locomotion—all occur in late Early and early Late Cretaceous (Albian–Cenomanian) *Wilbertopora*. The stratigraphic record of ovicells and avicularia appears to begin with *Wilbertopora*, whereas multiserial growth also occurs in the slightly older genus *Wawalia* Dzik, 1975. Prior to the appearance of *Wilbertopora*, the cheilostome record is marked by a long interval, spanning most of the Early Cretaceous, containing a low diversity of genera predominantly with uni- to pluriserial budding lacking cross-row communication pores (Taylor, 1986).

Although the presence of ovicells (Cheetham, 1954) and avicularia (Boardman and Cheetham, 1973; Cheetham, 1975) in *Wilbertopora* has been known for some time, the occurrence of zooids showing small morphological modifications apparently associated with enhancement of the operculum and associated musculature has until now gone unrecognized. Even though a variety of avicularian morphologies had been described previously, the general morphological similarity of non-avicularian zooids in colonies co-occurring with the type species, *W. mutabilis* Cheetham, 1954, led to the inclusion of a rather heterogeneous assemblage in this species (Boardman and Cheetham, 1973; Cheetham, 1975; Cheetham and Cook, 1983; Ostrovsky and Taylor, in press). Adding to the need for a complete revision of this assemblage is the growing realization, based on genetic and fine-scale morphometric evidence (Jackson and Cheetham, 1990, 1994; Herrera-Cubilla et al., in press), that many cheilostome morphospecies are seriously undersplit.

Here we undertake revision of the *Wilbertopora mutabilis* complex using the morphometric methods employed in the genetic-morphometric studies of living cheilostomes mentioned above, in order to provide as closely as possible an approximation to true biological species. Our analysis is limited to the type material of *W. mutabilis* and material that occurs in the same Albian–Cenomanian strata from which *W. mutabilis* sensu lato was originally collected in northeastern Texas and southeastern Oklahoma. Other, generally younger Cretaceous species that have been referred to *Wilbertopora*, either questionably (North Dakota, Cuffey et al., 1981) or more definitely (India, Taylor and Badve, 1994; Britain, Taylor, 2002), are not included in the present analysis.

SPECIMENS STUDIED AND THEIR STRATIGRAPHIC SETTING

All of the material studied was collected from the mid-Cretaceous Washita Group of northeastern Texas and southeastern Oklahoma (Fig. 1; Appendix 1). Most of the specimens are from two large collections: one made by H. T. Loeblich and A. Loeblich Jr. between 1937 and 1946, now housed in the Department of Paleobiology, National Museum of Natural History, Washington, DC (NMNH); the other made by M. Listokin in the late 1990s, now in the Department of Palaeontology, the Natural History Museum, London, England (NHM). Cheilostome bryozoans in these collections comprise several hundred specimens, all encrusting echinoid tests or mollusk shells, representing all of the eight formations in the Washita Group (Fig. 1; Cheetham, 1975, fig. 1). However, nearly all of the specimens from the lowermost formations, the Kiamichi and Duck Creek, are referable, not to *Wilbertopora* as emended below, but rather to uniserial to pluriserial genera such as *Pyriporopsis* Pohowsky, 1973, *Charixa*

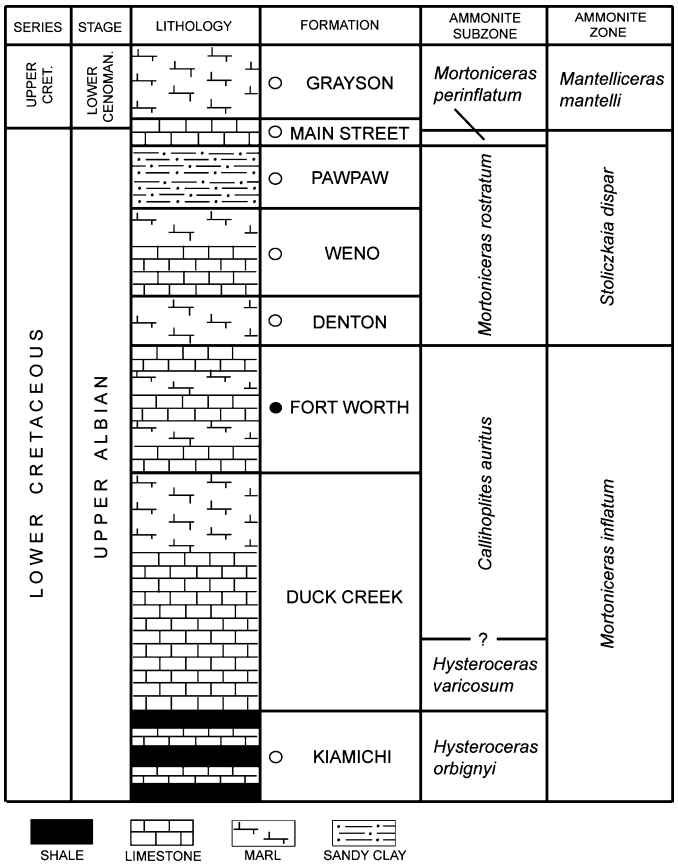

FIGURE *1*—Generalized stratigraphic column of Washita Group in northeastern Texas modified from Cheetham (1954) with European equivalent ammonite zones provided by A. S. Gale (personal commun., 2004). The interval from the Kiamichi Formation through the Main Street Formation is replaced toward the southwest by the Georgetown Formation, consisting of limestone and dolomite. Occurrences of *Wilbertopora* Cheetham, 1954 are shown by circles, the filled circle representing the type material of *W. mutabilis* Cheetham, 1954, the type species; occurrences of the new species described in this paper are shown in Table 2.

Lang, 1915, and *Spinicharixa* Taylor, 1986. In addition to specimens from these two collections, two smaller sets of specimens in the Department of Palaeontology, NHM, collected by C. Hoadley and by A. B. Smith and one of us (PDT), and in the Department of Paleobiology, NMNH, collected by N. E. Nelson, were included in the analyses below, along with the holotype of *W. mutabilis* borrowed from the Department of Geology and Geophysics, Louisiana State University, Baton Rouge (LSU). Locality data for all of this material are in Appendix 1.

A total of 93 *Wilbertopora* colonies have the requisite morphology for inclusion in the morphometric and subsequent cladistic analyses; these specimens include the holotypes of all the species and the paratypes of all the new species. An additional 55 colonies, although insufficiently preserved for morphometrics, were subsequently assignable to the species discriminated morphometrically; and a further 170 colonies, although assignable to *Wilbertopora*, are insufficiently preserved to identify to species.

Apart from the holotype of *Wilbertopora mutabilis*, the repositories for all the type and nontype material in this study are NMNH (catalogued under USNM numbers) and NHM.

DISCRIMINATION OF SPECIES

Methods.—To discriminate species in the *Wilbertopora mutabilis* complex, we first sorted the 93 colonies that possess the requisite features for morphometric analysis into eight groups qualitatively. The principal criterion for the initial sorting was avicularian morphology, particularly shape and relative size of the distal portion of the polymorph associated with the operculum or operculum equivalent (mandible). The range of avicularian morphologies comprises three groups in which the polymorphs show slight to moderate modifications of the morphology of the ordinary autozooids and five groups with variations of more typical avicularian form, with spatulate or pointed ends corresponding to mandibular shapes characteristic of many modern cheilostome bryozoans. The numbers of colonies in the eight groups vary from three to 35, with a median of seven.

To test the distinctiveness of the eight groups and the initial assignment of the 93 colonies to them, we employed a series of multivariate statistical procedures based on 26 metric characters of avicularia, ordinary autozooids, and the autozooids involved in brooding embryos (i.e., maternal zooids and their distal neighbors from which ovicells developed, including the ovicells themselves). These characters are explained in Appendix 2, and most are shown in Figure 2. Full use of the multivariate procedures requires measurement of at least one zooid of each type in each colony. However, zooids of some types, e.g., ordinary autozooids, are not associated with particular zooids of other types, e.g., avicularia, except through membership in a colony. Thus, the individual zooid data could not be used directly; instead, the basic data for the multivariate analyses are colony mean values (although all statistics in the species descriptions are based on the individual zooid measurements regardless of their grouping in colonies). To reduce statistical instability, we attempted to measure each character on three zooids per colony, but some characters could not be measured on even one zooid in some poorly preserved colonies. A further, and probably more important, precaution against instability was to limit measurements to zooids in zones of astogenetic repetition; ontogenetic variation is confined to less commonly preserved zooids at growing edges of colonies (e.g., Cheetham, 1975, pl. 3, fig. 1a, 1b) and thus was not an issue. Moreover, it must be emphasized that the degrees of freedom in the multivariate statistical tests employed here are all based on the numbers of colonies and variates, and thus not, at least directly, on the numbers of zooids. Operator error in measurements was minimized by employing electronic positioners attached to an X-Y stage with which specimens were moved under a stereomicroscope, and measurements digitally recorded on computer; all measurements were made by one of us (JS) who has much experience with this procedure and the equipment used.

The statistical procedures follow methods used in Cheetham (1986), Jackson and Cheetham (1994), Cheetham et al. (2001), and Herrera-Cubilla et al. (in press). The a priori groups were tested for their distinctiveness and for the ''correctness'' of assignments of colonies to them with discriminant function analysis calculated in the DISCRIMINANT procedure of SPSS 6.1 (Norusis, 1994b), with variables entering stepwise using Wilks's lambda as the criterion based on the default values of $P = 0.05$ to enter and $P = 0.10$ to remove. F-statistics calculated for each pair of groups have probabilities based on the numbers of cases (colonies in this study) in each of the groups, the total number of cases, and the number of variables (Norusis, 1994b, p. 27). We used $P < 0.001$ as the cutoff for distinctiveness between groups. ''Correctness of classification'' is based on whether the group to which the case (i.e., colony) was assigned is the one to which that case has the highest probability of belonging, given the function coefficients calculated in the stepwise analysis. All these criteria are identical to those employed in previous studies.

Results.—In an initial discriminant function analysis (DA) based on the 26 variates that are direct measurements (characters

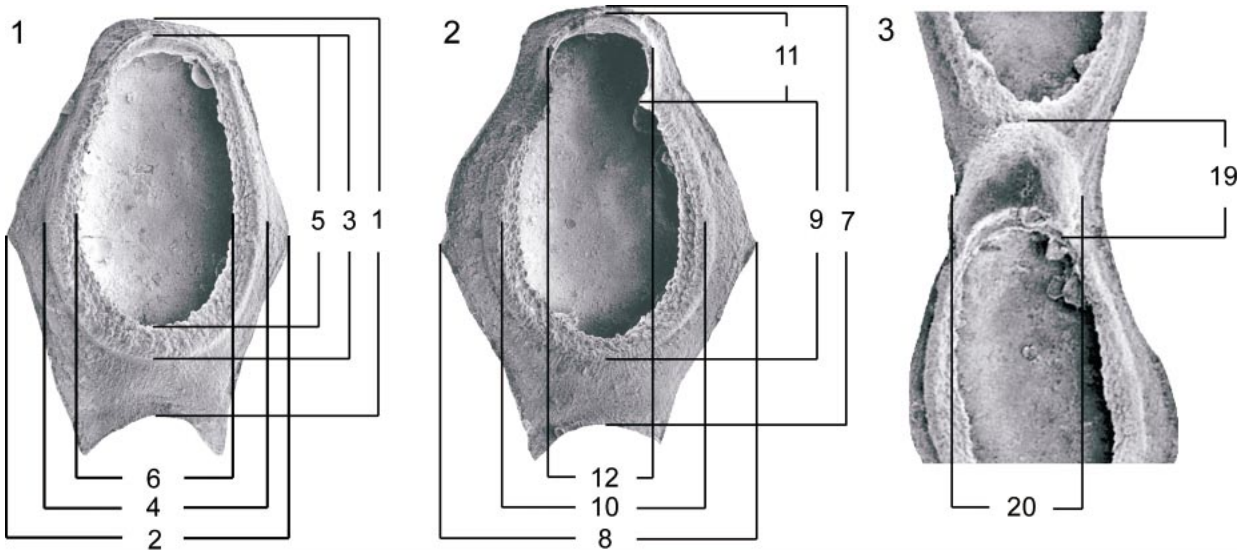

FIGURE 2—*1*, Ordinary autozooid showing measurement of characters 1–6. *2*, Avicularian polymorph, showing measurement of characters 7–12. *3*, Ovicell with distal part of maternal zooid and proximal part of distal, ovicell-bearing zooid, showing measurement of characters 19 and 20: characters 13–18 and 21–26 are not shown. Characters are numbered as in Appendix 2, where they are explained.

1–26, Appendix 2), only three characters (all avicularian measurements) contributed to discrimination (i.e., entered the stepwise analysis before discriminating power was exhausted, and were not subsequently removed), only six of the eight groups were distinct, and only 62% of the colonies were ''correctly classified'' (i.e., assigned to their highest probability groups). The poor resolution apparently resulted from the widespread occurrence of missing values in the data set (23%). Missing values prevent cases, and eventually, variates from entering the calculation of discriminant functions. However, the SPSS procedure DISCRIMINANT has a provision for substituting mean values in the classification phase of the analysis, i.e., when probabilities for membership in groups are calculated (Norussis, 1994b, p. 44). The grand means of each variate (i.e., means of colony means) provide the least biased estimates of missing values, so we made this substitution for a second DA. This procedure resulted in separation of all eight groups at $P < 0.001$ (all but two at $P < 0.0001$), 12 characters (half of which were avicularian metrics) contributing to the separation, and 93% of colonies ''correctly classified.''

For a third, and as it worked out, final DA, we added 34 ''shape'' characters to the data matrix by calculating ratios between various pairs of the original 26 measured characters (characters 27–60, Appendix 2). Here we included only ratios that have some obvious biological meaning, e.g., the ratio between the length and width of the distal part of the avicularian aperture (character 38) as a proxy for mandible shape; other possible ratios, such as avicularium length to autozooid width, without apparent meaning, were avoided. Although the introduction of these ratios can be expected to introduce redundancy because of their likely correlation with the original variates, the results suggest empirically that new discriminating power was gained by their addition. Again, we substituted grand means for missing ratios in this analysis. The new DA further improved upon the results of the second DA, bringing the percentage of colonies ''correctly classified'' to 100, making all eight groups distinct at the highest level of significance in F-tests ($P < 0.0001$, Table 1), and bringing the number of characters contributing to the separation of groups to 18, eight of which are ratios (Appendix 2). Nearly two-thirds (11 of 18) of the characters significant in this final DA involve avicularian measurements.

From these results, we infer that the eight groups (morphospecies, hereafter species) are equivalent to biological species distinguished with similar morphometric analyses in modern cheilostome bryozoan genera for which genetic data are available (Jackson and Cheetham, 1990, 1994; Herrera-Cubilla et al., in press). Overall morphological distances between species pairs (Table 1) range between 3.5 and 12.0, not a great difference given the large number of characters involved. Nevertheless, even in the reduced space of the first three discriminant axes (together accounting for 81% of the total variance), the overlap among species is slight, and three form completely distinct clusters (Fig. 3).

TABLE *1*—Discrimination of eight species of *Wilbertopora* based on 60 metric characters, of which 18 contributed significantly to the final DA (Appendix 2). *Above diagonal*, morphological distance, square root of Mahalanobis D^2. *Below diagonal*, F-value for multivariate distinctness, each with 18 and 68 degrees of freedom; all are significant at $P < 0.0001$. See text for further explanation.

	mutabilis	*listokinae*	*tappanae*	*spatulifera*	*attenuata*	*improcera*	*acuminata*	*hoadleyae*
mutabilis		7.293	8.346	8.487	11.671	7.943	10.945	10.831
listokinae	18.468		6.353	5.293	8.446	6.603	7.923	11.984
tappanae	6.865	5.035		8.660	11.020	8.224	11.975	11.876
spatulifera	18.850	16.054	8.9367		6.384	3.594	9.711	10.725
attenuata	18.935	14.098	10.287	7.437		5.720	8.260	11.784
improcera	12.667	15.322	7.051	3.954	4.927		8.176	9.532
acuminata	18.556	28.428	12.957	19.882	8.407	11.326		12.235
hoadleyae	16.306	28.388	11.948	20.987	15.684	13.684	18.444	

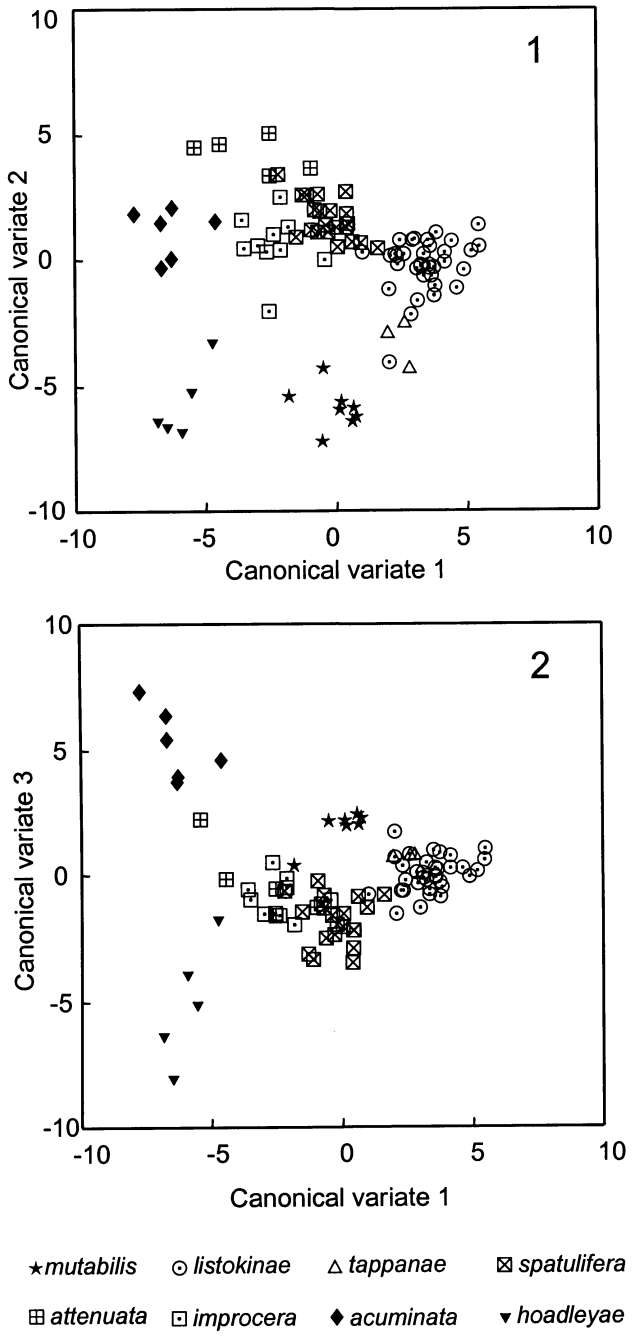

FIGURE 3—Plots of eight species of *Wilbertopora* on first three canonical axes from discriminant analysis based on 60 characters, together accounting for more than 80% of the total variance. *1*, Canonical variates 1 and 2. *2*, Canonical variates 1 and 3.

CLADISTIC ANALYSIS

Methods.—To estimate phylogenetic relationships among the eight species of the *Wilbertopora mutabilis* complex, we followed procedures employed in previous studies of cheilostome bryozoans (Jackson and Cheetham, 1994; Cheetham et al., 2001) and other taxa (e.g., Budd and Coates, 1992) that were based upon similar morphometric data. First, we tested all 60 characters for their statistical ability to distinguish among subsets of the eight species, using Duncan's Multiple Range test (DMRT) calculated with the SPSS routine ONEWAY (Norusis, 1994a). This procedure first calculates a standard single-classification analysis of variance (ANOVA) for each character based on an F-test of the differences among groups (species) with respect to within-group variation. Here we again used colony means as the basic data, but without substituting for missing values. DMRT then follows as a post-hoc test of which group means differ sufficiently (at a default significance level of $P < 0.05$) to form non-overlapping subsets of groups. Thus, this procedure may be regarded as a kind of ''gap coding.'' Even when group means differ at a very high level of significance in ANOVA, however, subsets from the subsequent post-hoc tests may overlap sufficiently that the character becomes ''uncodable'' and is dropped from further consideration. For this reason and also because existing programs require single-digit whole numbers for input, this form of coding is far from immune to the loss of resolution that plagues such methods. As a somewhat arbitrary compromise, we accepted subsets of species as distinct provided they overlapped by no more than one species. Each character with at least two such subsets was then coded for use in cladistic analysis. Coded states of each such character are assigned rank-order values in the range zero to nine, with the difference between successive states (ranks) equal to two for non-overlapping subsets or one with an overlap of one. Character 10 in Appendix 3 is an example of coding from three non-overlapping subsets, with 0 assigned for a mean value of 0.0802, 2 for means of 0.1145–0.1503, and 4 for means of 0.2173–0.2361. Character 5 in Appendix 3 is an example coded from two subsets overlapping by one group, 0.2615–0.2835 and 0.2835–0.3857.

Cladograms were calculated from the characters coded by DMRT for the eight species with PAUP* 4.0 (Swofford, 2000) and with Hennig 86 (Farris, 1988). Because the original data are all based on measurements, the characters were entered with ordered states. In both PAUP* 4.0 and Hennig 86, we used the search options that find all of the most parsimonious trees; this was only possible because there are fewer than 12 taxa.

To root the trees, we used *Wilbertopora mutabilis* sensu stricto, rather than choosing an outgroup taxon. *W. mutabilis* has by far the least differentiated avicularian polymorphs and is also one of the four clearly identifiable species of *Wilbertopora* with stratigraphic occurrences in the lower part of the Washita Group (correlative with the European *Mortoniceras inflatum* Zone, Fig. 1). Although a few colonies identifiable as *Wilbertopora* were found in the basal unit of the Washita Group, the Kiamichi Formation, they are too poorly preserved to assign to species, as discussed below. Given the importance of avicularian characters in discriminating species, there are no obvious outgroups of appropriate age from which to choose; other pre-Cenomanian species all lack avicularia.

Results.—Although the ANOVAs gave F-values significant at $P < 0.001$ for 31 of the 60 characters, only 20 were ''codable,'' i.e., separating the species into two or more subsets in the ensuing DMRTs (Appendix 3). For these characters, F-values were all significant at $P < 0.001$ (and all but four at $P < 0.0001$) (Appendix 3). The coding method described above yielded 79 states for the 20 characters. Thirteen of these characters are among the 18 significant in the final discriminant analysis, and 13 (all but one of which are among the characters significant in DA) involve avicularian measurements. Thus, agreement between the two statistical approaches is good, though inexact. However, only two out of seven non-avicularian characters significant in the DA yielded codable states in the DMRT. The matrix of coded states for the eight species is in Appendix 3.

Two maximally parsimonious trees were obtained with both PAUP* and Hennig 86 (Fig. 4), with length 122, consistency index 0.6721, and retention index 0.5604. Two of the 20 characters

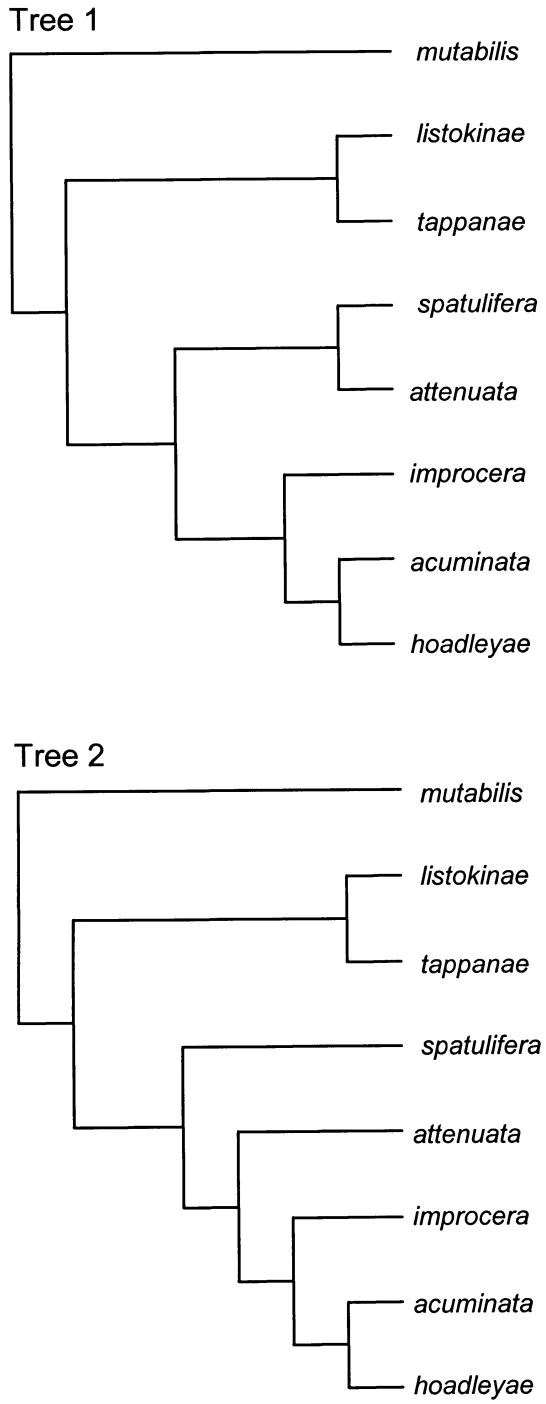

FIGURE 4—Two hypotheses of relationship among the eight species of *Wilbertopora*. The trees, rooted on *W. mutabilis*, are maximally parsimonious, with length 122, consistency index 0.6721, and retention index 0.5604. Trees, calculated in PAUP* (Swofford, 2000), were plotted in Treeview (Page, 1996).

are uninformative with regard to parsimony. One, the ratio between avicularium length and ordinary autozooid length (character 35), included three coded states and was also among the characters significant in DA; the other, the ratio between opesia length and aperture length in zooids distal to maternal zooids (character 59), included only two states and was not significant in DA. Without these two characters the consistency index of the trees is reduced to 0.6552.

The two trees agree in placing *W. listokinae* n. sp. and *W. tappanae* n. sp. within one clade and *W. spatulifera* n. sp., *W. attenuata* n. sp., *W. improcera* n. sp., *W. acuminata* n. sp., and *W. hoadleyae* n. sp. in another. The difference is whether or not *W. spatulifera* and *W. attenuata* form a subclade within this second clade. The stratigraphic occurrences of the species (Table 2) marginally favor the second tree, as *W. attenuata* appears in the record slightly after *W. spatulifera*.

Further assessment of the congruence of the second tree with the stratigraphic record is hampered by the coarseness of resolution (to formation only) and the poor preservation of the few specimens identifiable as *Wilbertopora* below the Fort Worth Formation (Table 2). Four of the eight species occur in the Fort Worth Formation, including two, *W. improcera* and *W. hoadleyae*, that are farthest from the root of the tree (Fig. 4); this strongly supports a hypothesis that all branching took place in the Fort Worth or earlier. However, that hypothesis requires long ghost ranges for two species, *W. listokinae* and *W. acuminata*, and shorter ones for two others, *W. tappanae* and *W. attenuata*; although sampling failure is not implausible, these range extensions are through the interval in which well-preserved specimens are common.

The key to resolving these discrepancies is undoubtedly in pre–Fort Worth deposits, so it is particularly unfortunate that only two colonies probably referable to *Wilbertopora* (and encrusting the same substrate) have been found lower in the section, in the Kiamichi Formation (Fig. 1). One of these extremely poorly preserved colonies appears to possess remnants of avicularia of two kinds, one similar to *W. tappanae* (Fig. 5.1) and the other more like those of *W. spatulifera* (Fig. 5.2); this colony could thus represent an ancestral condition preceding the first node in the tree (Fig. 4). The second colony lacks evidence of avicularia and consequently is not identifiable to species, even though its poorly preserved ovicells support its assignment to *Wilbertopora*. Although *W. tappanae* does not appear in the section until slightly later than *W. spatulifera* (Table 2), its avicularia are in many respects intermediate in morphology between those of *W. spatulifera* and *W. mutabilis*; thus, the occurrence of both types of avicularia together in a possible ancestor species does not seem implausible.

WILBERTOPORA AND THE EVOLUTION OF AVICULARIA

Avicularia as modified autozooids.—For much of the long history of bryozoology, the avicularian polymorphs so characteristic of the vast majority of cheilostome genera, both living and fossil, have been regarded as morphologically and functionally modified derivatives of the ordinary feeding zooids comprising the basic units of colonies. Banta (1973), Cook (1979), and Winston (1984, 1986, 1991) reviewed much of the evidence supporting this hypothesis, based on the skeletal morphology, soft-part anatomy, and behavior of living species. With the discovery of avicularium-like polymorphs in *Wilbertopora mutabilis* and the importance of avicularian characters in discriminating among its congeneric species, *Wilbertopora* assumes a new significance in exploring how the morphological transformation may have come about. Moreover, *Wilbertopora* is the only cheilostome whose known stratigraphic occurrence is consistent with any claim of priority for avicularian evolution. However, the similar series of morphologically modified zooids in genera with much more recent stratigraphic occurrences strongly suggest that avicularia may have evolved many times across a broad spectrum of cheilostome taxa, rather than being a direct legacy of their appearance in *Wilbertopora*.

Avicularia in cheilostomes are most commonly defined as zooids with an augmented opercular apparatus compared with that

TABLE 2—Numbers of colonies in formations of the Washita Group in northeastern Texas and southeastern Oklahoma assigned to each of the eight species of *Wilbertopora*. Numbers comprise all of the type and other material listed in the systematic paleontology section.

Formation	*mutabilis*	*listokinae*	*tappanae*	*spatulifera*	*attenuata*	*improcera*	*acuminata*	*hoadleyae*
Grayson		58					4	
Georgetown				4	2	4	1	
Main Street		1		5	1		4	
Paw Paw			1	3				
Weno			1					
Denton			3	5	3	6		
Fort Worth	13			16		5		8
Duck Creek								
Kiamichi			*	*				

* One of two poorly preserved specimens from the Kiamichi Formation has some characteristics suggesting assignment to *W. tappanae* n. sp. and *W. spatulifera* n. sp. combined in the same colony; see Figure 5.1 and 5.2 and text for discussion.

of co-occurring ordinary feeding autozooids. Augmentation in living species generally takes the form of: 1) thickening and other modifications of the cuticular operculum; 2) increase in size of the portion of the avicularium on which the mandible occludes relative to the pre-mandibular portion; 3) modification of the shape of the mandibular area to form a spatulate or acuminate rostrum (commonly with a skeletal shelf or palate against which the mandible occludes); 4) increase in the prominence of the skeletal hinge (usually condyles or a complete bar) that forms the fulcrum on which the mandible moves; 5) increase in the relative bulk of muscles that open and close the mandible; and 6) concomitant reduction of the lophophore and alimentary organs to a small setigerous organ presumed to serve a sensory function. Avicularia have been observed to fill a number of functional roles, including cleaning, defense, and support, but their morphology seems to be poorly correlated with behavior (e.g., reaction to stimulation) or with function (Cook, 1979). Moreover, skeletal morphology does not conform to the shape or size of the mandible in all cases, especially in species with setiform mandibles extending far beyond the margins of the avicularian skeleton.

The so-called B-zooids of *Steginoporella magnilabris* Busk, 1854, often taken as the starting point for models of avicularian differentiation, differ from the A-zooids in that species in having more strongly sclerotized opercula (presumably mandibles) with larger muscles. However, like the A-zooids, they have fully functional feeding organs and guts, and in fact may be the primary zooids appearing first in a developing colony (Cheetham and Jackson, personal data). Thus, a better model for understanding the morphology of avicularia in *Wilbertopora* may be in the more closely related genus *Crassimarginatella* Canu, 1900, in living species of which Cook (1968) has described a series of avicularian morphologies from slight modifications of the ordinary autozooids still retaining functional feeding organs to fully differentiated polymorphs lacking feeding ability (heterozooids).

Avicularian modification in Wilbertopora.—Avicularian mandibles have not been found in any species of *Wilbertopora*, and it must thus be assumed that they were at least initially much like the opercula of the ordinary feeding autozooids. Opercular morphology is preserved in calcified closure plates in one species, *W. listokinae*, especially among zooids in zones of astogenetic change (Fig. 6.1, 6.4). The opercula seem to have been simple flaps, with no evidence of appreciable thickening of their margins.

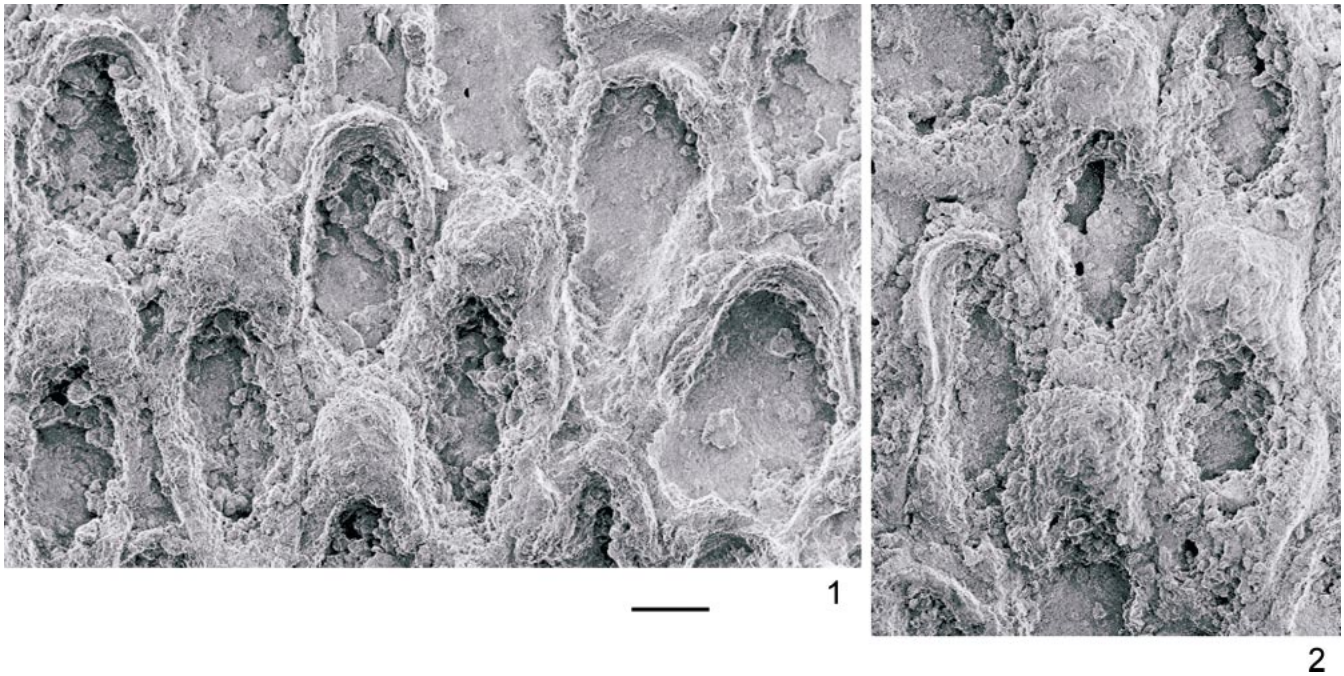

FIGURE 5—*Wilbertopora* sp., USNM 216144, HTL-170, Tarrant County, Texas, Kiamichi Formation, Upper Albian. *1*, Ordinary and ovicell-bearing autozooids, and three avicularia resembling those of *W. tappanae* n. sp. (see Fig. 9.5). *2*, Another part of same colony with ovicell-bearing autozooids and avicularium resembling those of *W. spatulifera* n. sp. (see Fig. 10.2). Scale bar 100 μm.

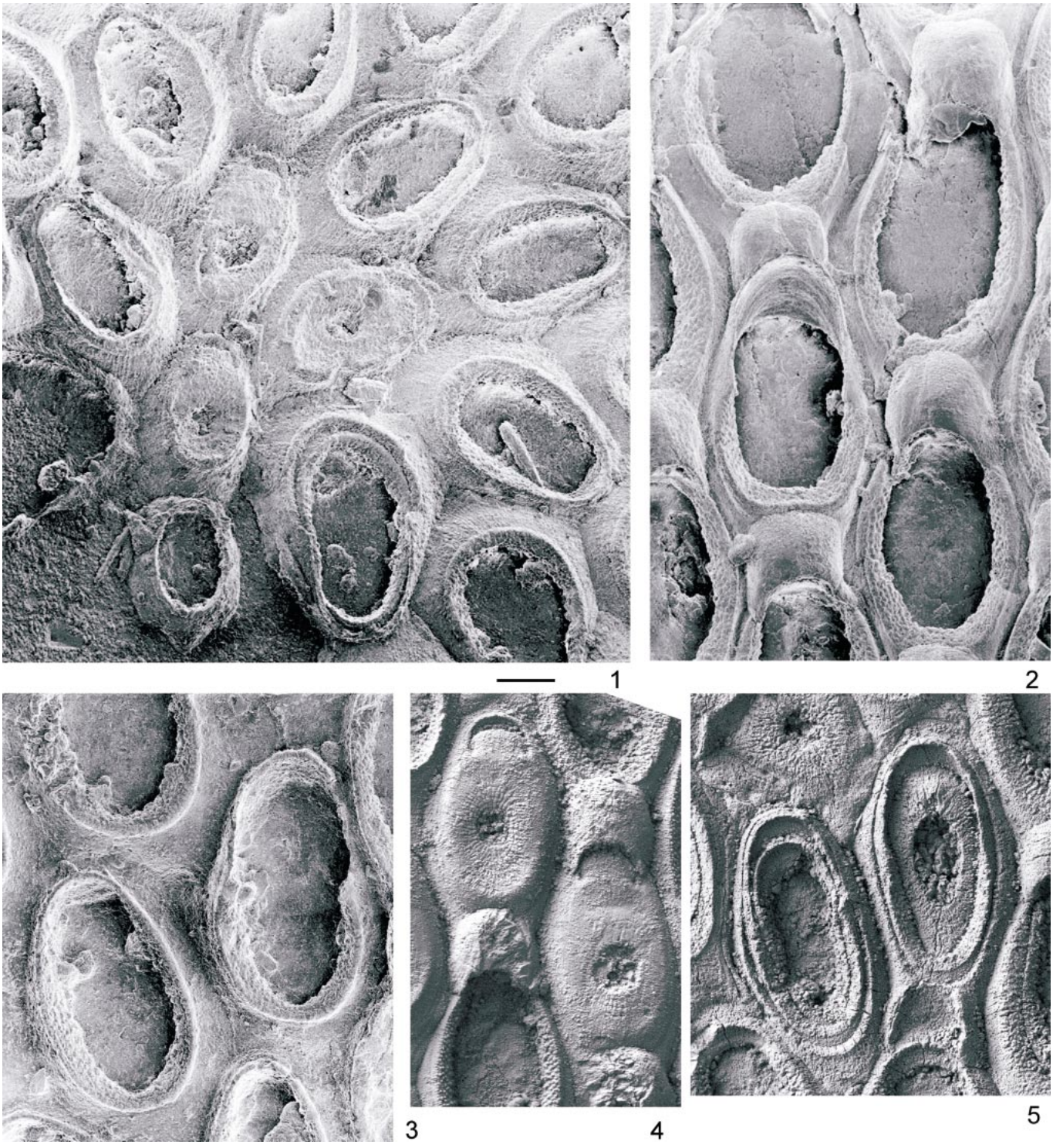

FIGURE 6—*Wilbertopora listokinae* n. sp., Grayson County, Texas, Grayson Formation, Lower Cenomanian. *1*, Paratype, USNM 216140, HTL-5, ordinary autozooids in zone of astogenetic change, three with closure plates, and ordinary autozooids, one budded intramurally, in zone of repetition. *2*, Holotype, USNM 216175, HTL-5, ovicell-bearing and maternal autozooids, and one avicularium proximal to ovicell and apparently occluding its opening. *3*, Paratype, USNM 526269, HTL-5, ordinary autozooid and avicularium. *4*, Paratype, NHM BZ1856(1), ordinary and ovicell-bearing autozooids with calcified closure plates. *5*, Paratype, NHM BZ1627, two ordinary autozooids within which other zooids have been budded intramurally, one with a calcified closure plate. Scale bar 100 μm.

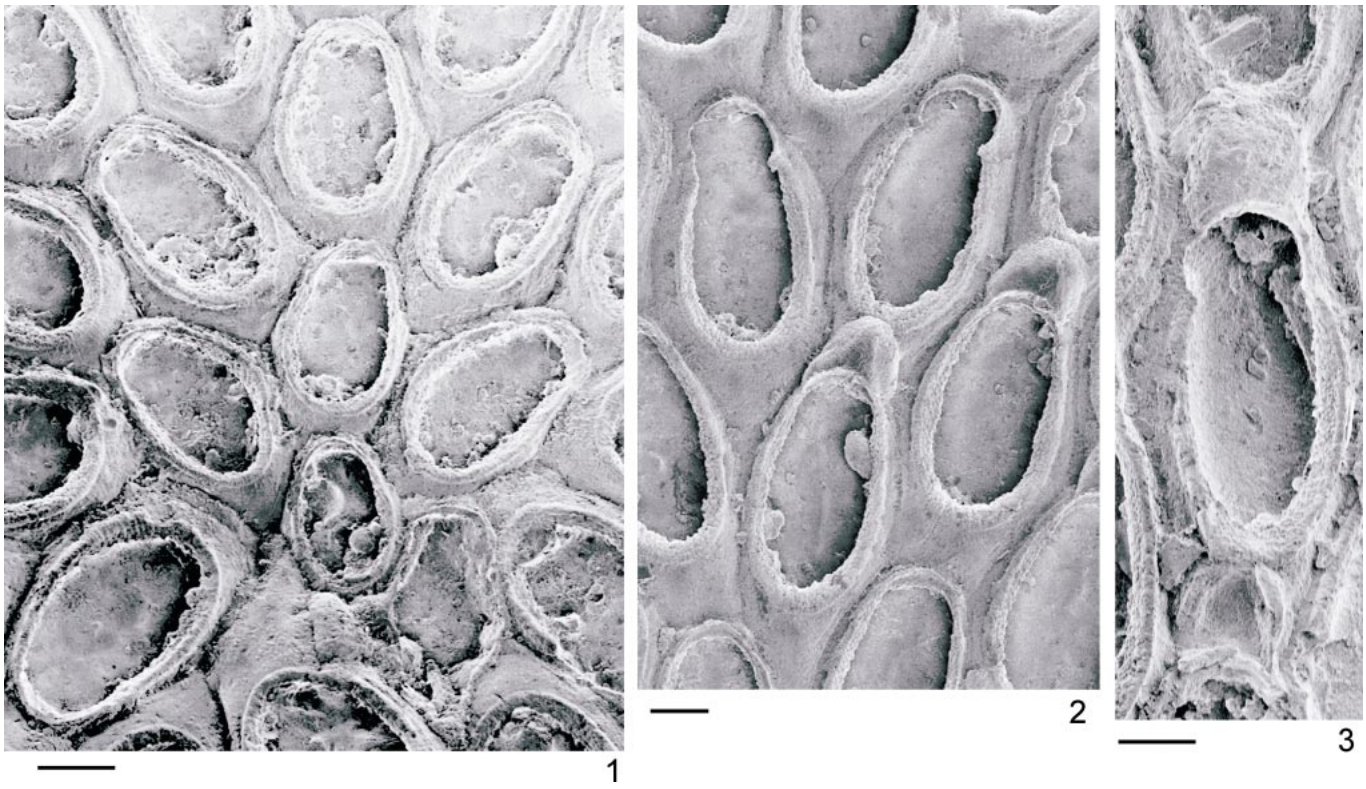

FIGURE 7—*Wilbertopora mutabilis*, Fort Worth Formation, Upper Albian. *1*, Holotype, LSU 4500, Denton County, Texas; ordinary autozooids, zone of astogenetic change. *2*, Holotype, LSU 4500, Denton County, Texas; ordinary autozooids, avicularian polymorphs, and two ovicells, one of which is developed on a polymorph. *3*, USNM 216155, HTL-67, Marshall County, Oklahoma; avicularian polymorph that apparently also served as a maternal autozooid; note partially developed (or broken) ovicell on its proximal gymnocyst. Scale bars 100 μm.

Neither *W. listokinae* nor any of the other seven species of *Wilbertopora* shows any evidence of modification of the underlying calcareous skeleton of the ordinary feeding autozooids to suggest that the operculum was hinged on skeletal condyles or knobs.

The least modified stage of avicularian differentiation appears in *W. mutabilis* in the form of distinct inflections of the lateral gymnocyst to form supports for hinging the operculum (Figs. 2.2, 7.2, 7.3). There is no evidence, however, to indicate whether the operculum remained a simple flap or was reinforced by additional sclerotization. These avicularium-like polymorphs in *W. mutabilis* remained functional autozooids (i.e., with lophophores), as shown by their intermittent occurrence as maternal zooids at the proximal opening of ovicells, developed in all species of *Wilbertopora* as outgrowths from the proximal gymnocyst of the distally neighboring zooid (Fig. 7.3). Development of an ovicell and deposition of embryos in it, according to Silén (1945), require a maternal zooid that possesses a lophophore, at least a rudimentary gut, and an ovary; the lophophore and gut may be otherwise nonfunctional, as in *Celleporella* Gray, 1848 (see Marcus, 1938; Ryland and Gordon, 1977).

The gymnocystal inflections on which the operculum hinged divide the zooidal aperture (i.e., the skeletal margin of the frontal membrane) in *W. mutabilis* into distinct distal and proximal portions (characters 11 and 9, Fig. 2 and Appendix 2). The mean ratio between the lengths of these portions is just under 0.35 (Fig. 7.2), approximately equal to the ratio between opercular and preopercular lengths in the feeding autozooids of *W. listokinae* that have closure plates (Fig. 6.1, 6.4). Together, these characteristics suggest that these polymorphs in *W. mutabilis* were even less differentiated from the ordinary autozooids than those of the living species *Crassimarginatella similis* Cook, 1968, which retained apparently functional lophophores and alimentary organs (Cook, 1968).

Evidence for augmentation of the opercular apparatus of avicularian polymorphs is much more pronounced in the other seven species of *Wilbertopora*. The ratio between distal and proximal portions of the aperture increases to more than 0.5 in all cases (Fig. 8.1), averaging about 1.0 (i.e., approximately evenly divided), although with much variation in this proportion (approaching as much as 2.0 in *W. attenuata*). *Crassimarginatella similis* appears to fit in the low end of this range [approximately 0.6 in fig. 18 of Cook (1968)], as do species of the subgenus *Crassimarginatella* (*Corbulella*) Gordon, 1984 described and illustrated by Gordon (1984, pl. 3, e; pl. 4, b); the avicularia of these species may be fully functional autozooids, like those in *C. similis*, i.e., with feeding organs, but such organs have not been explicitly reported.

Although completely distinct from *W. mutabilis* in relative lengths of distal portions of their avicularian apertures, the other seven species exhibit little if any pattern in the variation of this ratio with increasing distance from *W. mutabilis* in the cladistic tree (Fig. 8.1). However, if all of the six measurements of avicularian dimensions are included in a measure of deviation from mean values in *W. mutabilis* (Fig. 8.2), a trend becomes apparent. The trend is highly significant (Spearman correlation 0.742, $P < 0.001$ with 78 degrees of freedom). Among the qualitative changes paralleling this trend are: 1) appearance of a small shelf on the distal margin of the avicularian aperture in *W. listokinae* and *W. tappanae* (Figs. 6.2, 6.3, 9.3, 9.5) that expands proximally to form a calcified palate on which the mandible occluded in *W. spatulifera* (Fig. 10.1, 10.2), *W. attenuata* (Fig. 11.1, 11.2), *W. improcera* (Fig. 12.2, 12.3), *W. acuminata* (Fig. 13.2), and *W. hoadleyae* (Fig. 14.1, 14.2); 2) accentuation of the lateral gymnocystal

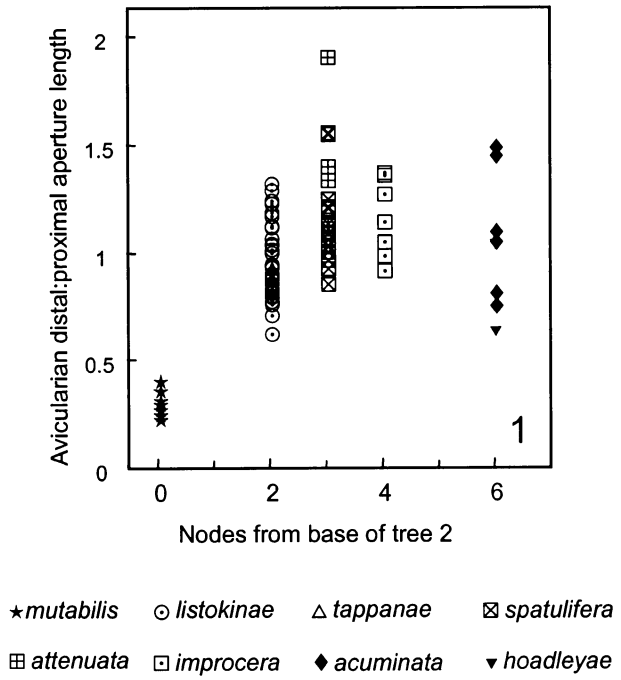

FIGURE 8—Differentiation of avicularia in eight species of *Wilbertopora* plotted against position in cladistic tree. *1,* Ratio between distal aperture length and proximal aperture length of avicularia or avicularium-like polymorphs; mean values, *W. mutabilis*, 0.3246; *W. listokinae* n. sp., 0.9865; *W. tappanae* n. sp., 0.9107; *W. spatulifera* n. sp., 1.1520; *W. attenuata* n. sp., 1.4621; *W. improcera* n. sp., 1.1778; *W. acuminata* n. sp., 1.1230; *W. hoadleyae* n. sp., 0.8672. *2,* Deviation (sum of squared deviations in six avicularian measurements) from mean vector of *W. mutabilis.*

inflections separating the distal and proximal portions of the avicularian apertures, seen in *W. mutabilis*, *W. listokinae*, and *W. tappanae* (Figs. 6.2, 7.2, 9.5), to form more prominent hinging structures for the mandible in *W. spatulifera*, *W. attenuata*, *W. improcera*, *W. acuminata*, and *W. hoadleyae* (Figs. 10.1, 11.1, 12.3, 13.2, 14.2); and 3) various changes in the overall shape of the distal portion of the avicularian aperture, perhaps reflecting changes in mandible shape, although the caveat of Cook (1979) regarding the far from exact congruence between mandible and underlying skeletal structures applies to the probability of any such conclusion.

Like the polymorphs of *W. mutabilis*, the avicularia of *W. listokinae* may have possessed functional lophophores; they occur intermittently proximally to zooids bearing ovicells on their proximal gymnocysts; however, in some cases at least, the avicularia appear to have formed by intramural budding, perhaps replacing a damaged maternal zooid, or the ovicell appears to have aborted, perhaps because the requisite organs of the potential maternal zooid were aborted (Fig. 6.2). Similar occurrences in *W. spatulifera* (Fig. 10.3) and *W. improcera* (Fig. 12.3) appear even less likely to represent use of an ovicell by an avicularium, the distal margin of which seems to block the ovicell opening or the ovicell is greatly reduced in size, again perhaps reflecting aborted development of requisite organs. The proportions of the distal portion of the avicularian apertures in *W. tappanae* also make it possible that these polymorphs possessed functional lophophores, although none have been found proximal to ovicells. For *W. attenuata*, avicularia seem even less likely to have had functional lophophores, and the highly modified avicularia of *W. acuminata* and *W. hoadleyae* almost surely lacked lophophores.

The clear gradient of morphological changes in these eight species of *Wilbertopora* thus parallels in greater detail that described by Cook (1968) in living species of *Crassimarginatella*. If this pattern was indeed the first occurrence of such a trend, as the known stratigraphic record suggests, it could be the template on which avicularian evolution was repeated in other cheilostome taxa through Late Cretaceous and Cenozoic time.

SYSTEMATIC PALEONTOLOGY

Family CALLOPORIDAE Norman, 1903
Genus WILBERTOPORA Cheetham, 1954

Wilbertopora CHEETHAM, 1954, p. 179.

Type species.—Wilbertopora mutabilis Cheetham, 1954.

Diagnosis (emended herein).—Colonies forming encrusting sheets of usually a single layer of zooids arranged more or less quincuncially and communicating within and across budding rows through pore chambers and pore plates. Zooids polymorphic. Ordinary autozooids rounded hexagonal to elliptical in frontal view, with the frontal membrane-operculum complex occupying distal three-fourths of zooid length and medial three-fourths of zooid width, and a narrow, smooth gymnocyst comprising the remaining proximal and lateral areas; cryptocyst a narrow, finely pustulose, slightly concave, inwardly sloping ledge on the lateral and proximal margins of the distinct mural rim defining an elliptical to ovoid aperture; opesia with similar shape and almost same size as aperture; few small oral, and rarely, lateral spines present in some species. Avicularia or avicularium-like polymorphs present in all species, interzooidal and, depending on species, ranging from zooids very similar to ordinary autozooids to fully differentiated avicularia with rounded, spatulate, or acuminate distal portions and condyles or complete pivotal bar. Ovicell a small, prominent, globular chamber roofed by two flattened spinelike folds completely calcified on both inner and outer surfaces and meeting medially to form a suture; folds emanate from uncalcified openings in slightly elongated, concave proximal gymnocyst of distal zooid forming floor of brood chamber; ovicell-bearing zooid can be otherwise ordinary autozooid, avicularian polymorph, or kenozooid; ovicell opens proximally at distal margin of proximally adjoining zooid, presumably the maternal zooid; maternal zooid an ordinary autozooid or, in some cases in some species, an avicularian polymorph. Ancestrula a smaller, but otherwise ordinary autozooid, giving rise to either a single distal bud or a distal and two distolateral buds; post-ancestrular

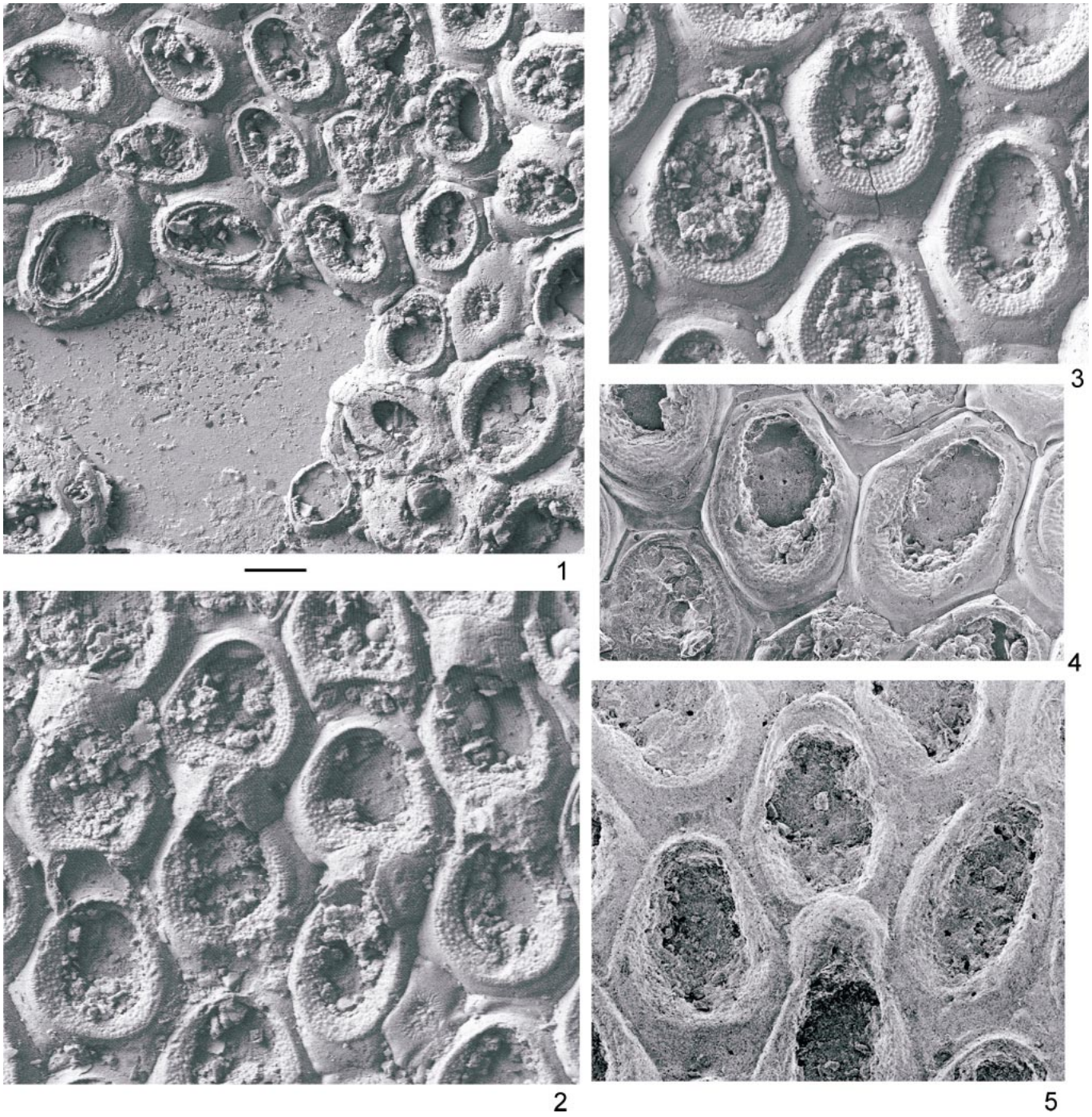

FIGURE 9—*Wilbertopora tappanae* n. sp., Upper Albian. *1,* Paratype, NHM BZ1124 a, Bryan County, Oklahoma, Weno Formation; autozooids in zone of astogenetic change, and autozooids (some with intramural buds) and kenozooid in zone of repetition. *2,* Holotype, NHM BZ1124 c, Bryan County, Oklahoma, Weno Formation; ordinary and ovicell-bearing autozooids and kenozooid in zone of repetition. *3,* Holotype, NHM BZ1124 c, Bryan County, Oklahoma, Weno Formation; autozooid and avicularium, zone of repetition. *4,* Paratype, USNM 526290, HTL-81, Cook County, Texas, Denton Formation; autozooids with spine bases. *5,* USNM 526291, Denton County, Texas, Paw Paw Formation; avicularium bearing ovicell on proximal gymnocyst, and autozooids. Scale bar 100 μm.

zooids increase gradually over a few generations, forming together with the ancestrula a distinct zone of astogenetic change; polymorphs generally appear in the succeeding zone of astogenetic repetition.

Occurrence.—Washita Group, Upper Albian–Lower Cenomanian, northeastern Texas-southeastern Oklahoma; Bagh Beds, Cenomanian(?)–Coniacian(?), central India; British Chalk, Turonian–Campanian, southern England;? Fox Hills Sandstone, Maastrichtian, North Dakota.

Discussion.—The Washita Group *Wilbertopora* species are remarkably similar in morphology of ordinary feeding autozooids

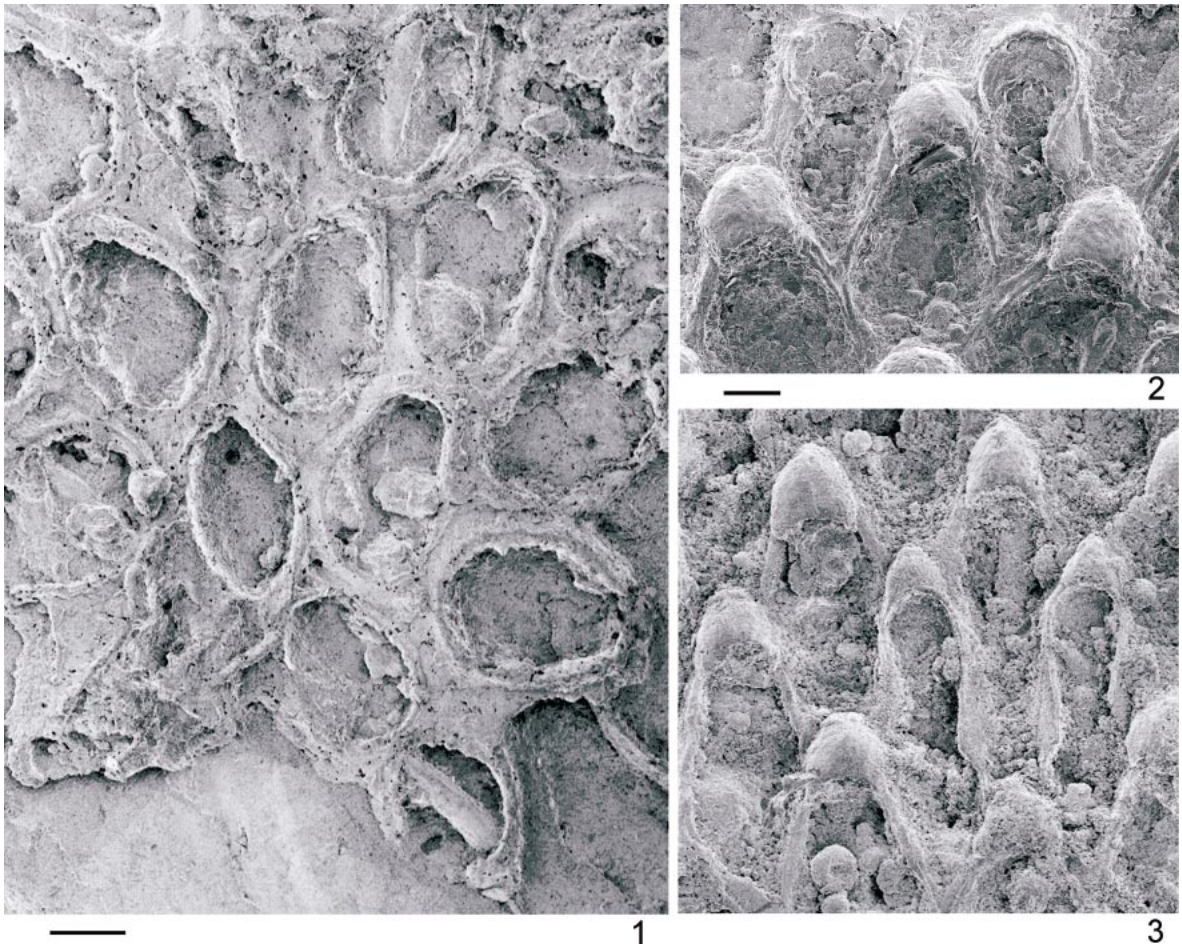

FIGURE *10—Wilbertopora spatulifera* n. sp., Upper Albian. *1,* Paratype, USNM 526305, HTL-96, Williamson County, Texas, Georgetown Formation; zone of astogenetic change and part of zone of repetition, with ordinary autozooids and one avicularium. *2,* Holotype, USNM 526292, HTL-9, Grayson County, Texas, Fort Worth Formation; autozooids, ovicells, and avicularia, zone of repetition. *3,* Paratype, USNM 526296, HTL-41, Tarrant County, Texas, Fort Worth Formation; ''normal'' ovicells distal to autozooids and reduced (nonfunctional?) ovicells distal to two avicularia. Scale bars 100 μm.

and ovicells, differing mostly in avicularian morphology. The younger Cretaceous species assigned to this genus by Taylor and Badve (1994), *W. blanfordi* (Guha, 1989) from the Bagh Beds of India, and by Taylor (2002), *W. woodwardi* (Brydone, 1910) from the British Chalk, appear also to fit this pattern, although pore chambers were not explicitly described in these species. Pore chambers (also known as dietellae) are a conspicuous feature of the Washita Group species of *Wilbertopora* and were apparently inherited from their morphologically simpler predecessors, including the Late Jurassic *Pyriporopsis* (Banta, 1975). If the Indian and British species do indeed belong to *Wilbertopora*, they appear to represent more extreme points in the evolution of spatulate and acuminate avicularia, respectively.

Ovicell development in *Wilbertopora* has been described in detail by Ostrovsky and Taylor (in press).

In the absence of avicularian polymorphs, the Washita Group species of *Wilbertopora* are virtually indistinguishable. As a result, a total of 170 colonies in the collections studied could not be assigned to species.

WILBERTOPORA MUTABILIS Cheetham, 1954
Figure 7

Wilbertopora mutabilis CHEETHAM, 1954, p. 180, pl. 20, figs. 1–3; BOARDMAN AND CHEETHAM, 1969, pl. 30, fig. 2; BOARDMAN AND CHEETHAM, 1973, fig. 39, a; CHEETHAM, 1975, pl. 2, fig. 1; CHEETHAM AND LORENZ, 1976, fig. 21; CHEETHAM AND COOK, 1983, fig. 80.3; TAYLOR, 1988, fig. 5b.

Diagnosis (emended herein).—Avicularium-like polymorphs with apertures divided into distinct distal and proximal portions by slight inflections of lateral gymnocyst, forming rudimentary condyles to pivot presumed mandible; distal portion approximately one-third as long and nearly two-thirds as wide as proximal portion; avicularian polymorphs otherwise differ little in size, shape, or proportions from ordinary autozooids.

Description.—Colonies start with an ancestrula, about 50% as large as zooids in zones of repetition, that gives rise directly to three zooids emanating one from distal pore chamber and one from each distolateral pore chamber; succeeding zooids increase in size gradually for two or three generations, arising from the distal and one or both of the distolateral pore chambers of the preceding zooid. Zooidal basal walls calcified. Ordinary autozooids hexagonal to elliptical, averaging just over 0.5 mm long and just over 0.3 mm wide, widest near midlength; gymnocyst smooth, slightly convex except in zooids on which ovicells are developed, somewhat broader proximally than laterally; mural rim sharp and prominent, enclosing an oval to elliptical aperture that occupies the distal 75% of zooid length and the medial 75% of

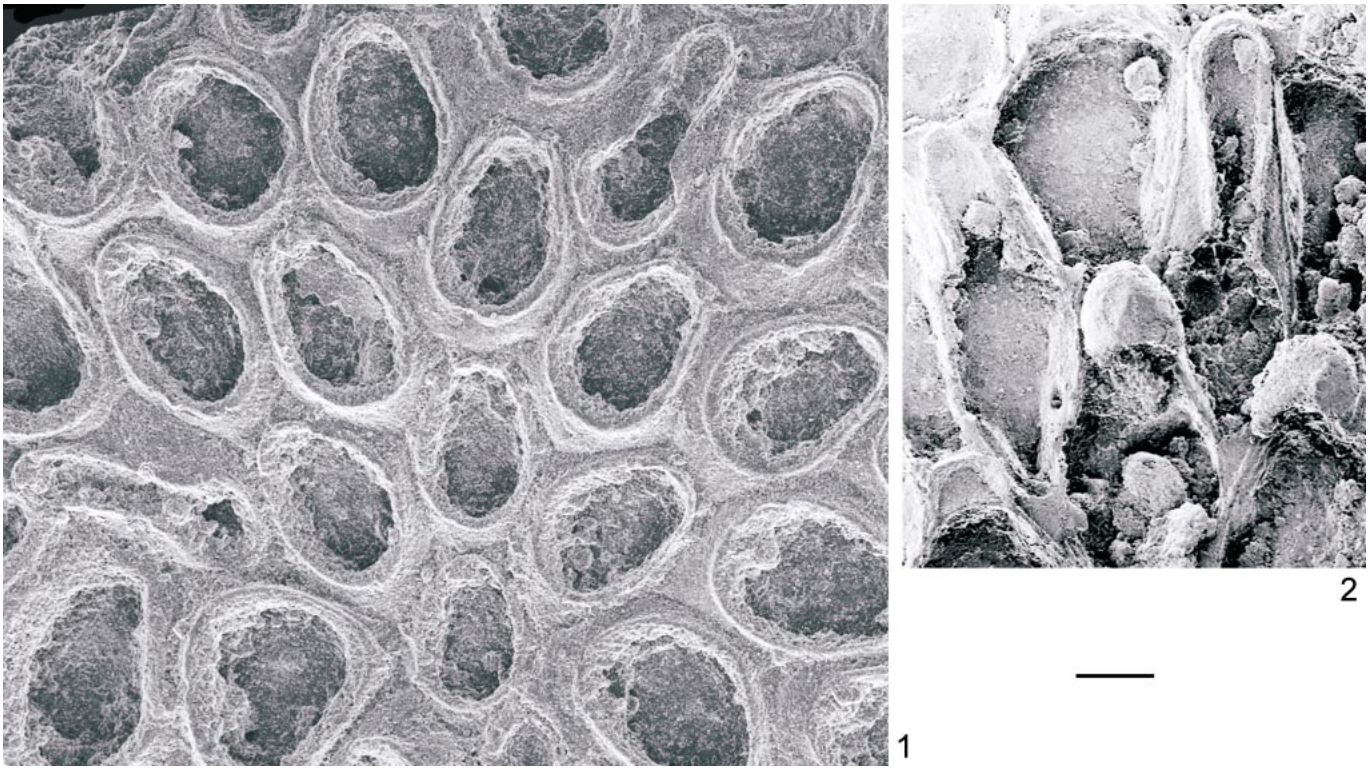

FIGURE *11*—*Wilbertopora attenuata* n. sp., Upper Albian. *1*, Holotype, USNM 526319, HTL-99, Johnson County, Texas, Denton Formation; zone of astogenetic change and part of zone of repetition with ordinary autozooids and two avicularia. *2*, Paratype, USNM 526323, HTL-96, Williamson County, Texas, Georgetown Formation; ovicells, maternal autozooids, and two avicularia. Scale bar 100 μm.

zooid width; cryptocyst a crescent-shaped ledge, slightly broader proximally than laterally, sloping inward, with a finely pustulose surface; opesia similar in shape to aperture, occupying nearly 90% of aperture length and 75% of aperture width; oral spines not seen. Avicularium-like polymorphs occur in zones of repetition, approximately same size and shape as ordinary autozooids with similar gymnocyst and cryptocyst, but mural rim inflected medially on each side at presumed proximolateral corners of operculum-equivalent to form pivot, giving aperture a distinctly pinched outline; distal portion approximately 25% of total aperture length and 60% of aperture width; distal rim slightly more elevated and arcuate than that of ordinary autozooid, but not otherwise significantly different. Ovicells limited to zones of repetition, formed on proximal portion of gymnocyst of zooid distal to maternal zooid; both maternal and ovicell-bearing zooids can be either ordinary autozooids or avicularium-like polymorphs; gymnocyst of ovicell-bearing zooid slightly concave to serve as floor of brood chamber; ovicell surface similar to that of gymnocyst, with faint median suture discernible in some specimens; ovicell opening arcuate. Small kenozooids can occur in budding pattern or as intramural buds; some autozooids can be developed intramurally as well.

Material examined.—LSU 4500 (holotype), USNM 651282, NHM D47068 (topotypes); USNM 216150, USNM 526254, HTL-56; USNM 216153, HTL-48; USNM 216155, USNM 526255, HTL-67; USNM 526256, HTL-9; USNM 526257, USNM 526258, HTL-39.

Measurements.—See Table 3.

Occurrence.—Upper Albian. Fort Worth Formation, Love, Marshall, and Choctaw counties, Oklahoma; Cooke, Grayson, Denton, Tarrant, and Johnson counties, Texas.

Discussion.—The avicularium-like polymorphs of *W. mutabilis* are similar enough to ordinary autozooids that their presence in the holotype of this species has gone unnoticed until now. A consequence has been the inclusion of material with more distinct avicularia in this species, ultimately with forms having both spatulate and acuminate avicularia, described below, lumped together as conspecifics (Cheetham and Cook, 1983). Closer observation also shows that all the material examined possesses thinly calcified basal zooidal walls, contrary to the original description (Cheetham, 1954), although the encrusted substrate commonly shows through. Also, as pointed out by Cheetham (1975), the original description misinterpreted a case of intramural budding in the holotype as the introduction of a second type of ovicell (Cheetham, 1954).

W. mutabilis appears to be the only one of the eight Washita Group *Wilbertopora* species in which the avicularium-like polymorphs most probably possessed functional lophophores capable of depositing embryos in the ovicells which commonly occur on zooids distal to them; although ovicells occur in other species in similar positions with respect to avicularia, morphological evidence suggests that they probably were reproductively nonfunctional.

WILBERTOPORA LISTOKINAE new species
Figure 6

Wilbertopora mutabilis; CHEETHAM, 1975, pl. 2, fig. 2; pl. 3, fig. 1; CHEETHAM AND COOK, 1983, figs. 80.1, 80.4.

Diagnosis.—Avicularia with apertures divided into distinct distal and proximal portions by slight inflections of lateral gymnocyst, as in *W. mutabilis*, but distal portion approximately as long and nearly as wide as proximal portion, with more broadly arcuate and raised distal margin and moderately developed distal shelf,

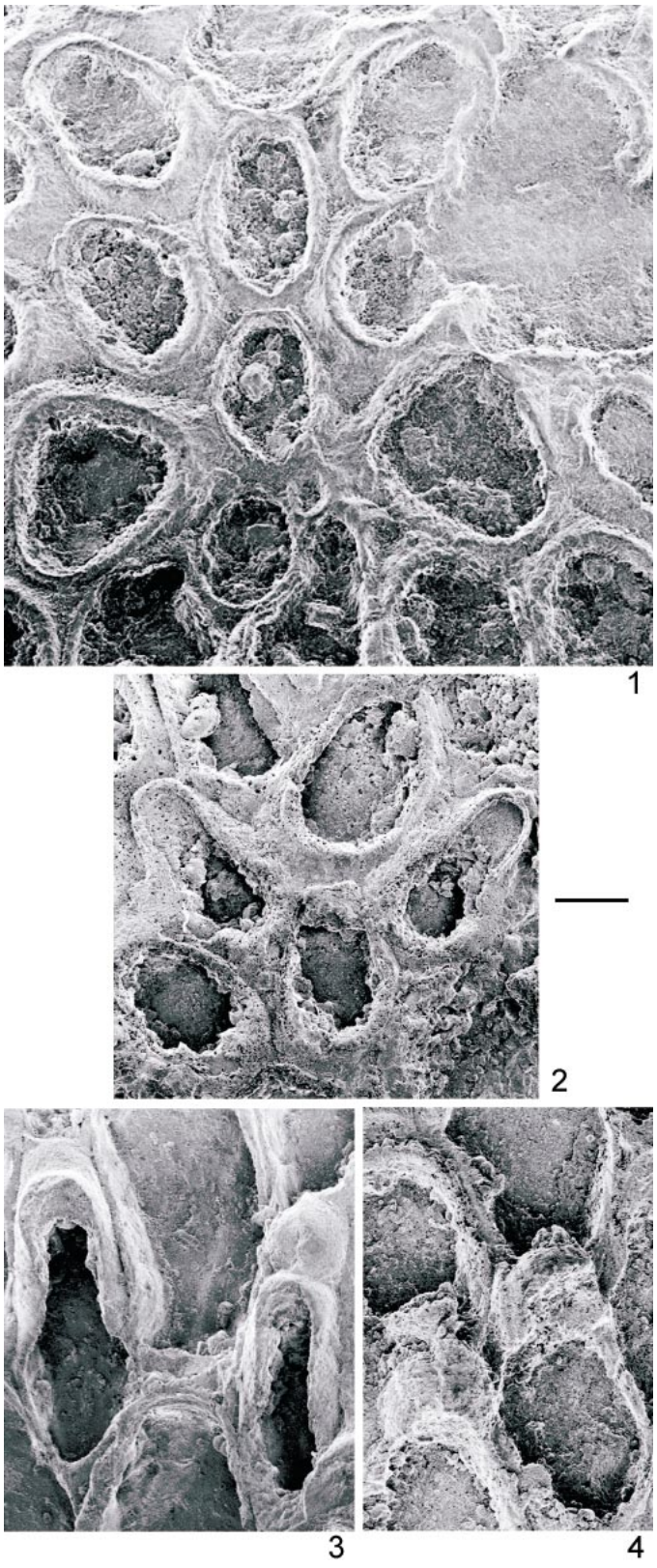

FIGURE 12—*Wilbertopora improcera* n. sp., Upper Albian. *1*, Paratype, USNM 526329 HTL-96, Williamson County, Texas, Georgetown Formation; autozooids, zone of astogenetic change. *2*, Holotype, USNM 216163, HTL-25, Grayson County, Texas, Denton Formation; ordinary autozooids and two avicularia. *3*, Paratype, USNM 216152, HTL-48, Cooke County, Texas, Fort Worth Formation; avicularia, one of which apparently occluded ovicell at its distal margin. *4*, Paratype, USNM 526327, HTL-43, Tarrant County, Texas, Fort Worth Formation; maternal and ovicell-bearing autozooids. Scale bar 100 μm.

but otherwise differing little in size or shape from ordinary autozooids.

Description.—Colonies start with an ancestrula, about 45%–50% as large as zooids in zones of repetition, that gives rise to a single zooid emanating from distal pore chamber; succeeding zooids arise from distal and one or both distolateral pore chambers, increasing in size gradually for two or three generations. Zooidal basal walls calcified. Ordinary autozooids rounded hexagonal to elliptical, averaging just under 0.6 mm long and just over 0.3 mm wide, widest near midlength; gymnocyst smooth, slightly convex except in zooids on which ovicells are developed, somewhat broader proximally than laterally; mural rim sharp and prominent, enclosing an oval to elliptical aperture that occupies the distal 75%–80% of zooid length and the medial 75%–80% of zooid width; cryptocyst a crescent-shaped ledge, slightly broader proximally than laterally, sloping inward, with a finely pustulose surface; opesia similar in shape to aperture, occupying approximately 90% of aperture length and 80% of aperture width; up to four very small oral spine bases present in few zooids in both zones of change and zones of repetition; frontal closure plates preserving flaplike operculum common, especially in zones of change; surface finely pustulose, resembling texture of cryptocyst. Avicularia occur in zones of repetition or in few cases by intramural budding in zooids in zones of change; slightly longer than ordinary autozooids, but about the same width and similar in shape and with similar gymnocyst and cryptocyst; inflection of marginal gymnocyst not as pronounced as in *W. mutabilis*, giving aperture a less pinched outline; distal portion 50% of total aperture length and 85% of aperture width; distal rim slightly more elevated and much more arcuate than that of ordinary autozooid, with up to four very small spine bases in few zooids, and a steeply sloping, relatively broad, concave distal shelf. Ovicells limited to zones of repetition, formed on proximal portion of gymnocyst of zooid distal to maternal zooid; both maternal zooid and distal zooid can be either ordinary autozooids or avicularia, although if apparent maternal zooid is an avicularium, the ovicell appears aborted in development, or its opening is partly or completely covered by raised distal margin of the avicularium; ovicell-bearing zooid can also be a kenozooid in rare cases; gymnocyst of ovicell-bearing zooid slightly concave to serve as floor of brood chamber; ovicell surface similar to that of gymnocyst, commonly with median suture or a raised median ridge; ovicell opening either arcuate or inverted V-shaped. Both intramural budding and closure plates common.

Etymology.—Named for Monica Listokin.

Types.—Holotype USNM 216175, paratypes USNM 216140, USNM 216174, USNM 216177, USNM 526259–USNM 526262, HTL-5; paratypes USNM 216141, USNM 526263–USNM 526273, NHM BZ1699, NHM BZ1700, HTL-1; paratype USNM 526274, HTL-8; paratype USNM 526275, HTL-31; paratype USNM 216171, HTL-45; paratypes USNM 526276–USNM 526278, HTL-87; paratype USNM 526279, HTL-90; paratype USNM 526280, HTL-103; paratypes NHM BZ1614, NHM BZ1856, NHM BZ1912, NHM D58502, NHM D57378, NHM D58508.

Measurements.—See Table 3.

Other material examined.—USNM 216278, USNM 216279 b, c, USNM 526281–USNM 526285, HTL-1; USNM 526286–USNM 526288, HTL-5; USNM 216173, HTL-8; USNM 216172

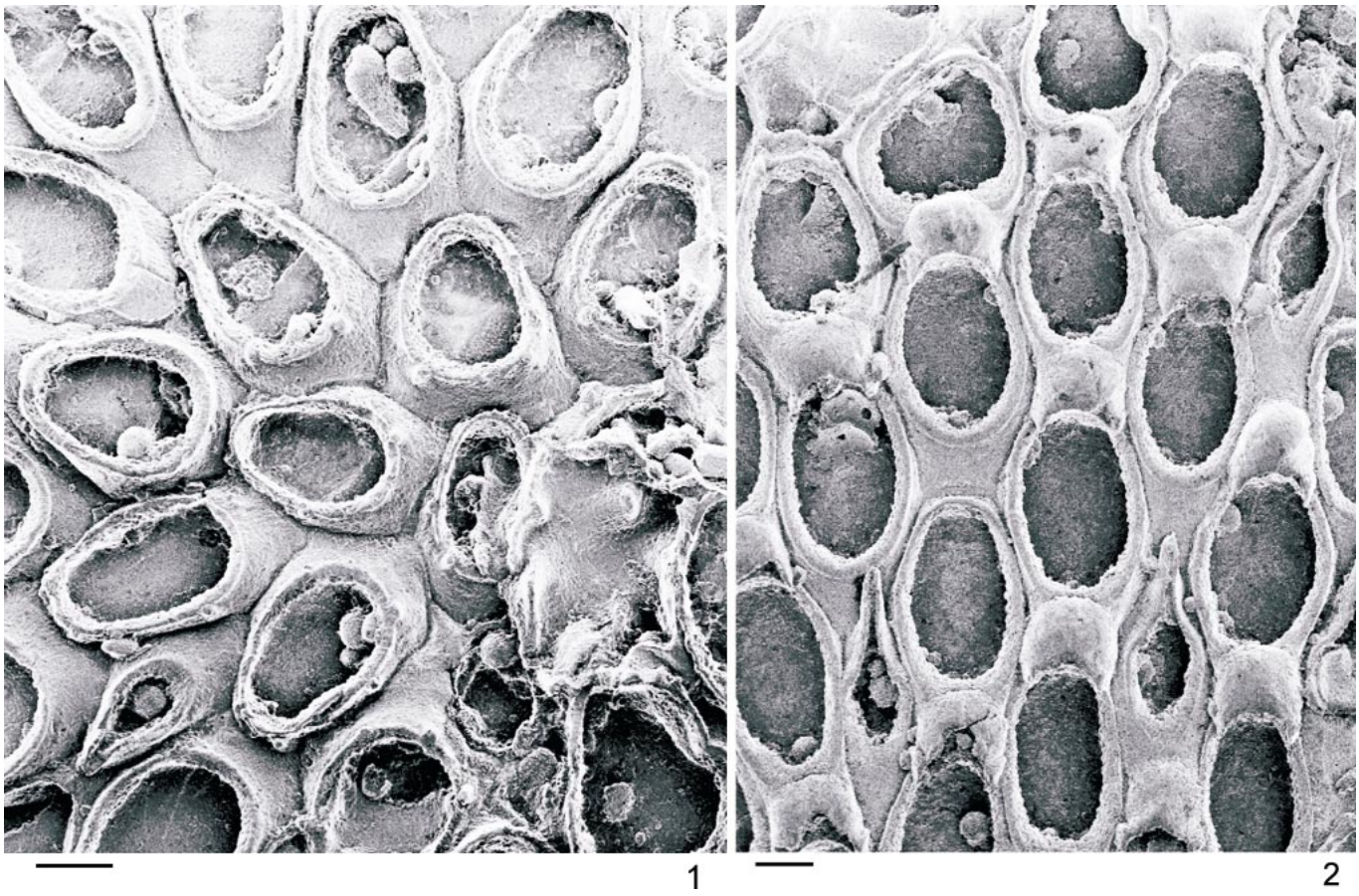

FIGURE *13*—*Wilbertopora acuminata* n. sp., holotype, USNM 216143, HTL-89, Bell County, Texas, Grayson Formation, Lower Cenomanian. *1*, Ordinary autozooids, zone of astogenetic change and autozooids and avicularium, zone of repetition; *2*, autozooids and avicularia; ovicells borne on proximal gymnocysts of numerous autozooids and those of two avicularia (upper and lower right). Scale bars 100 μm.

b, c, d, e, HTL-87; NHM BZ1352, NHM BZ1627, NHM D58503, NHM PEI 49.

Occurrence.—Lower Cenomanian, Main Street Formation, Tarrant County, Texas; Grayson Formation, Bryan County Oklahoma; Grayson, Denton, Tarrant, Johnson, McLennan, Bell, and Travis counties, Texas.

Discussion.—*W. listokinae* is the only one of the Washita *Wilbertopora* species in which calcified closure plates and intramural budding (''regeneration'' or ''reparative budding'') are common. Although ovicells occur on zooids distal to some avicularia in this species, this occurrence may not indicate that avicularia possessed functional lophophores because of their association with intramural budding and other evidence of disturbance of the growth pattern.

WILBERTOPORA TAPPANAE new species
Figure 9

Diagnosis.—Avicularia with apertures divided into distal and proximal portions of approximately same length, as in *W. listokinae* n. sp., but distal margin less broadly arcuate and raised. Both ordinary autozooids and avicularia 20%–25% smaller than in *W. mutabilis* and *W. listokinae*.

Description.—Ancestrular region poorly preserved, but ancestrula about 50% as large as zooids in zones of repetition; succeeded by one or possibly two zooids each budded serially from a distal pore chamber, followed by distally and distolaterally budded zooids, increasing in size gradually for two or three generations. Zooidal basal walls calcified. Ordinary autozooids rounded hexagonal to elliptical, averaging just over 0.4 mm long and just under 0.3 mm wide, widest near midlength; gymnocyst smooth, slightly convex, only slightly wider proximally than laterally; mural rim rounded, usually less prominent than in *W. mutabilis* and *W. listokinae*, enclosing a roughly oval aperture that occupies the distal 70%–75% of zooid length and the medial 70%–75% of zooid width; cryptocyst a crescent-shaped ledge, slightly broader proximally than laterally, sloping inward, with a finely pustulose surface; opesia somewhat more elliptical than aperture, occupying approximately 85% of aperture length and 75% of aperture width; up to four very small oral spine bases present in some zooids. Avicularia approximately same size and shape as ordinary autozooids, with similar gymnocyst and cryptocyst; inflection of marginal gymnocyst less pronounced than in *W. mutabilis*, giving aperture a less pinched outline; distal portion slightly less than 50% of total aperture length and 80% of aperture width; distal rim slightly more elevated and slightly more arcuate than that of ordinary autozooid, without oral spines, with a steeply sloping, narrow, concave distal shelf. Ovicells formed on proximal portion of gymnocyst of zooid distal to maternal zooid, which is an ordinary autozooid; distal zooid also, except possibly in one case, an autozooid; gymnocyst of ovicell-bearing zooid slightly concave to serve as floor of brood chamber; ovicell surface similar to that of gymnocyst, with a raised median ridge in better-preserved specimens; ovicell opening arcuate.

Etymology.—Named for Helen Tappan Loeblich.

Types.—Holotype NHM BZ1124 c, paratype NHM BZ1124 a; paratypes USNM 526289, USNM 526290, HTL-81.

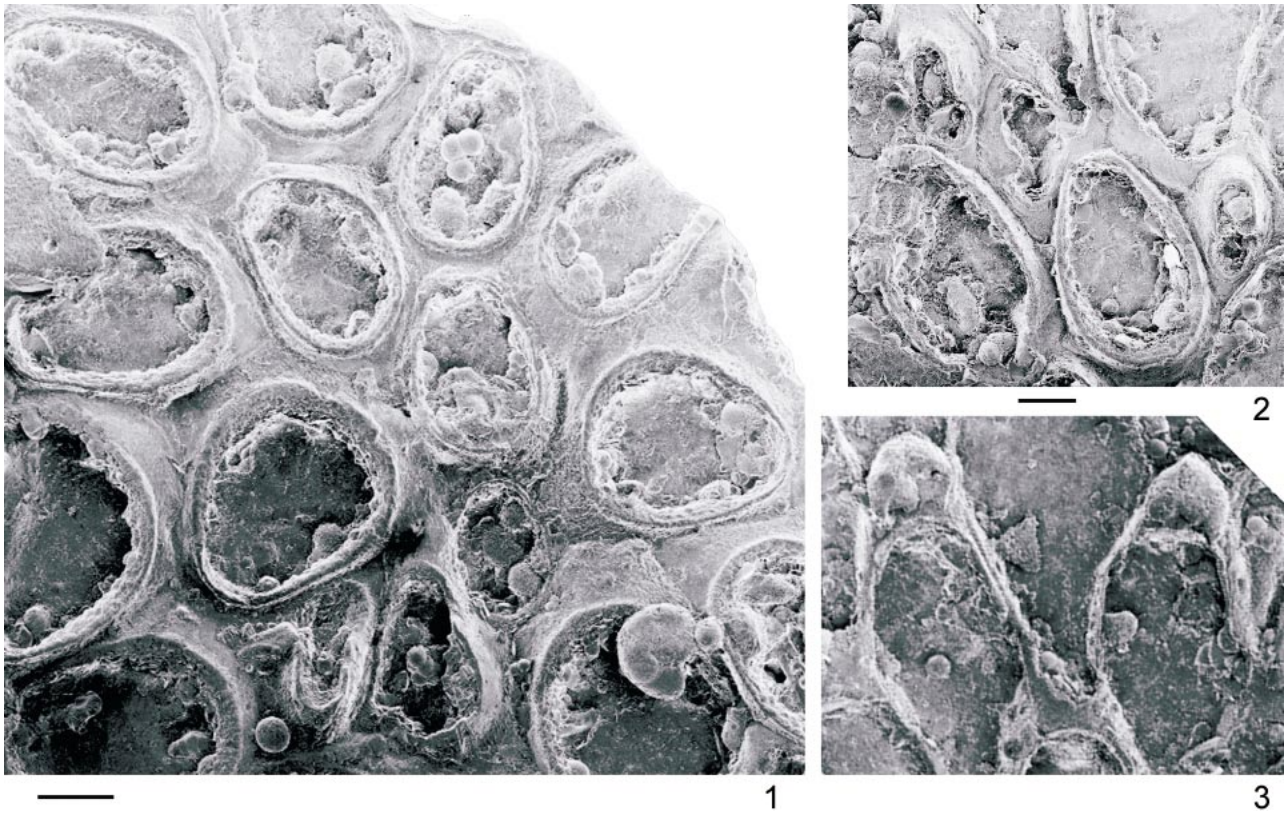

FIGURE *14*—*Wilbertopora hoadleyae* n. sp., holotype, USNM 526341, HTL-9, Grayson County, Texas, Fort Worth Formation, Upper Albian. *1*, Zone of astogenetic change and part of zone of repetition with ordinary autozooids and an avicularium. *2*, Ordinary autozooids and three avicularia. *3*, Maternal autozooids and ovicells. Scale bars 100 μm.

Measurements.—See Table 3.

Other material examined.—USNM 216159, HTL-33; USNM 526291.

Occurrence.—Upper Albian, Denton Formation, Cooke and Grayson counties, Texas; Weno Formation, Bryan County, Oklahoma; Paw Paw Formation, Tarrant County, Texas.

Discussion.—*W. tappanae* is one of three Washita Group *Wilbertopora* species having small zooids and avicularia. It is also one of the less common species; well-preserved specimens are especially rare.

WILBERTOPORA SPATULIFERA new species
Figure 10

Wilbertopora mutabilis; BOARDMAN AND CHEETHAM, 1973, fig. 40, c; CHEETHAM, 1975, pl. 3, fig. 2; CHEETHAM AND COOK, 1983, fig. 81.4.

Diagnosis.—Avicularia almost 10% longer and about 15% narrower than ordinary autozooids, with apertures divided into distal and proximal portions of approximately same length by strong inward inflections of lateral gymnocyst; distal margin flared in spatulate shape, with extensive, slightly sloping shelf forming mandibular palate.

Description.—Colonies start with an ancestrula, about 45%–50% as large as zooids in zones of repetition, that gives rise to a single zooid emanating from distal pore chamber; succeeding zooids arise from distal and one or both distolateral pore chambers, increasing in size gradually for two or three generations. Zooidal basal walls calcified. Ordinary autozooids rounded hexagonal to elliptical, averaging well over 0.5 mm long and just under 0.3 mm wide, widest near midlength; gymnocyst smooth, slightly convex except in zooids on which ovicells are developed, broader proximally than laterally; mural rim sharp and prominent, enclosing an oval to elliptical aperture that occupies the distal 80%–85% of zooid length and the medial 85%–90% of zooid width; cryptocyst a crescent-shaped ledge, slightly broader proximally than laterally, sloping inward, with a finely pustulose surface; opesia similar in shape to aperture, occupying approximately 90% of aperture length and 80% of aperture width; oral spines not seen. Avicularia distinctly longer and slightly narrower than ordinary autozooids, but otherwise of similar shape; gymnocyst smooth, strongly inflected laterally, but not forming distinct pivotal condyles; cryptocyst a very narrow ledge at proximal margin of aperture; distal portion slightly more than 50% of total aperture length and equal to total aperture width; distal rim slightly more elevated than that of ordinary autozooid, moderately to strongly flared into spatulate shape, with a gently sloping, broad distal shelf forming mandibular palate. Ovicells formed on proximal portion of gymnocyst of zooid distal to maternal zooid, which is an ordinary autozooid; rarely, zooids distal to avicularia have greatly reduced, apparently nonfunctional ovicells; gymnocyst of ovicell-bearing zooid slightly concave to serve as floor of brood chamber; ovicell surface similar to that of gymnocyst, with a raised median ridge in better-preserved specimens; ovicell opening arcuate.

Etymology.—Latin, *spatula*, diminutive of *spathe*, a broad blade, and *fero*, to bear, in allusion to the shape of the distal portion of the avicularian aperture.

Types.—Holotype USNM 526292, paratype USNM 216154, HTL-9; paratype USNM 526293, HTL-11; paratype USNM 526294, HTL-14; paratype USNM 526295, HTL-25; paratype USNM 526296, HTL-41; paratypes USNM 186572, USNM

TABLE 3—Measurements (mm) of Washita Group *Wilbertopora* species.

	W. mutabilis	*W. listokinae*	*W. tappanae*	*W. spatulifera*
Number of colonies measured	8	35	3	21
Ordinary autozooids				
Number measured	16	69–70	7–9	6–46
Length, mean	0.5194	0.5545	0.4229	0.5379
Standard deviation	0.0332	0.0819	0.0333	0.0855
Width, mean	0.3211	0.3185	0.2988	0.2805
Standard deviation	0.0450	0.0486	0.0370	0.0421
Aperture length, mean	0.4071	0.4353	0.3057	0.4187
Standard deviation	0.0264	0.0626	0.0126	0.0503
Aperture width, mean	0.2448	0.2473	0.2152	0.2516
Standard deviation	0.0272	0.0327	0.0217	0.0323
Opesia length, mean	0.3613	0.3892	0.2613	0.3784
Standard deviation	0.0283	0.0588	0.0096	0.0484
Opesia width, mean	0.1929	0.1894	0.1597	0.1915
Standard deviation	0.0207	0.0305	0.0138	0.0304
Avicularian polymorphs				
Number measured	14	72	3	39–56
Length, mean	0.5333	0.5775	0.4276	0.5838
Standard deviation	0.0741	0.0885	0.0258	0.1080
Width, mean	0.3034	0.3179	0.3027	0.2340
Standard deviation	0.0423	0.0408	0.0342	0.0417
Proximal aperture length, mean	0.3074	0.2391	0.1814	0.2423
Standard deviation	0.0484	0.0451	0.0153	0.0699
Proximal aperture, width, mean	0.2214	0.2354	0.2173	0.1505
Standard deviation	0.0207	0.0303	0.0036	0.0250
Distal aperture length, mean	0.0988	0.2346	0.1648	0.2578
Standard deviation	0.0105	0.0347	0.0067	0.0426
Distal aperture, width, mean	0.1368	0.1996	0.1726	0.1570
Standard deviation	0.0136	0.0243	0.0205	0.0244
Ovicells				
Number measured	21	100	6	34–35
Length, mean	0.1604	0.1850	0.1613	0.1593
Standard deviation	0.0102	0.0223	0.0133	0.0210
Width, mean	0.1712	0.1843	0.1633	0.1711
Standard deviation	0.0144	0.0373	0.0238	0.0185

526297, HTL-43; paratype USNM 216157b, HTL-47; paratypes USNM 526298, USNM 526299, HTL-48; paratype USNM 526300, HTL-54; paratype USNM 526301, HTL-56; paratype USNM 526302, HTL-67; paratype USNM 526303, HTL-85; paratype USNM 216170 a, HTL-86; paratypes USNM 526304, USNM 526305, HTL-96; paratypes USNM 526306, USNM 526307, HTL-99; paratype NHM BZ1372.

Measurements.—See Table 3.

Other material examined.—USNM 526308, HTL-48; USNM 526309, HTL-53; USNM 526310, HTL-54; USNM 216168, USNM 526311, HTL-55; USNM 526312, HTL-56; USNM 526313, HTL-67; USNM 526314, HTL-85; USNM 526315, HTL-86; USNM 526316, HTL-201; USNM 526317, HTL-225; USNM 526318; NHM BZ1123, NHM BZ1125.

Occurrence.—Upper Albian, Fort Worth Formation, Love, Marshall, and Choctaw counties, Oklahoma; Cooke, Grayson, Denton, Tarrant, and Johnson counties, Texas; Denton Formation, Grayson, Tarrant, and Johnson counties, Texas; Weno Formation, Bryan County, Oklahoma; Pawpaw Formation, Tarrant County, Texas. Lower Cenomanian, Main Street Formation, Tarrant, Johnson, and Bell counties, Texas; Georgetown Formation, Williamson and Travis counties, Texas.

Discussion.—Its much more distinctly differentiated avicularia distinguish *W. spatulifera* from all the preceding species, and the more flared distal portions of its avicularia from all the following ones. Although it is one of the commonest and most widely occurring of the Washita Group *Wilbertopora* species, well-preserved specimens are rare.

WILBERTOPORA ATTENUATA new species
Figure 11

Diagnosis.—Avicularia similar to those in *W. spatulifera*, but 20%–25% longer and 20% narrower than ordinary autozooids; distal portion of avicularian aperture about 40% longer than proximal portion and only slightly to moderately flared in spatulate shape; distal shelf extends about halfway to gymnocystal inflections to form mandibular palate.

Description.—Colonies start with an ancestrula, about 50% as large as zooids in zones of repetition, that gives rise directly to three zooids, one emanating from distal pore chamber and one from each distolateral pore chamber; succeeding zooids increasing in size gradually for two or three generations. Zooidal basal walls calcified. Ordinary autozooids rounded hexagonal to elliptical, averaging slightly less than 0.5 mm long and slightly more than 0.25 mm wide, widest near midlength; gymnocyst smooth, slightly convex except in zooids on which ovicells are developed, slightly broader proximally than laterally; mural rim sharp and prominent, enclosing an oval to elliptical aperture that occupies the distal 75%–80% of zooid length and the medial 75%–80% of zooid width; cryptocyst a crescent-shaped ledge, slightly broader proximally than laterally, sloping inward, with a finely pustulose surface; opesia similar in shape to aperture, occupying approximately 90% of aperture length and 80% of aperture width; oral spines not seen. Avicularia 20%–25% longer and 20% narrower than ordinary autozooids, with a more elongate elliptical shape; gymnocyst smooth, strongly inflected laterally, but not forming distinct condyles; cryptocyst a moderately broad, crescent-shaped ledge extending about a third the length of the proximal portion

TABLE 4—Measurements (mm) of Washita Group *Wilbertopora* species.

	W. attenuata	*W. improcera*	*W. acuminata*	*W. hoadleyae*
Number of colonies measured	5	10	6	5
Ordinary autozooids				
Number measured	5–15	6–30	9–10	3–14
Length, mean	0.4819	0.4659	0.4167	0.4996
Standard deviation	0.1060	0.0509	0.0400	0.0535
Width, mean	0.2774	0.2720	0.2448	0.3107
Standard deviation	0.0558	0.0313	0.0186	0.0345
Aperture length, mean	0.3747	0.3736	0.3236	0.3915
Standard deviation	0.0350	0.0339	0.0290	0.0350
Aperture width, mean	0.2141	0.2086	0.2081	0.2696
Standard deviation	0.0245	0.0197	0.0225	0.0351
Opesia length, mean	0.3365	0.3334	0.2798	0.3346
Standard deviation	0.0317	0.0299	0.0327	0.0799
Opesia width, mean	0.1754	0.1701	0.1651	0.2284
Standard deviation	0.0128	0.0166	0.0179	0.0371
Avicularian polymorphs				
Number measured	11–15	15–26	18	5–15
Length, mean	0.5956	0.4730	0.4220	0.2828
Standard deviation	0.0999	0.0681	0.0531	0.0563
Width, mean	0.2218	0.2088	0.1539	0.1732
Standard deviation	0.0459	0.0219	0.0184	0.0309
Proximal aperture length, mean	0.2202	0.1863	0.1461	0.0969
Standard deviation	0.0621	0.0398	0.0208	0.0153
Proximal aperture, width, mean	0.1425	0.1303	0.1145	0.0889
Standard deviation	0.0124	0.0231	0.0127	0.0180
Distal aperture length, mean	0.3077	0.2057	0.1599	0.0901
Standard deviation	0.0623	0.0517	0.0317	0.0380
Distal aperture, width, mean	0.0989	0.1069	0.0440	0.0675
Standard deviation	0.0237	0.0204	0.0075	0.0078
Ovicells				
Number measured	11	15	16	9
Length, mean	0.1407	0.1447	0.1523	0.1557
Standard deviation	0.0188	0.0168	0.0197	0.0234
Width, mean	0.1494	0.1583	0.1750	0.1653
Standard deviation	0.0142	0.0173	0.0570	0.0080

of the aperture; distal portion slightly more than 60% of total aperture length and about 70% of total aperture width; distal rim slightly more elevated than that of ordinary autozooid, almost straight to moderately flared into spatulate shape, with a gently sloping, distal shelf extending about halfway to gymnocystal inflections to form mandibular palate. Ovicells formed on proximal portion of gymnocyst of zooid distal to maternal zooid, which is an ordinary autozooid; gymnocyst of ovicell-bearing zooid slightly concave to serve as floor of brood chamber; ovicell surface similar to that of gymnocyst, with a faint median suture; ovicell opening arcuate.

Etymology.—Latin, *attenuatus*, drawn out, tapered, in allusion to the shape of the distal portion of the avicularian aperture.

Types.—Holotype USNM 526319, HTL-99; paratype USNM 526320, HTL-25; paratype USNM 526321, HTL-54; paratype USNM 526322, HTL-96; paratype NHM BZ2275.

Measurements.—See Table 4.

Other material examined.—USNM 526323, HTL-37; USNM 526324, HTL-96.

Occurrence.—Upper Albian, Denton Formation, Grayson and Johnson counties, Texas. Lower Cenomanian, Georgetown Formation, McLennan and Williamson counties, Texas.

Discussion.—*W. attenuata* is distinctive among the Washita Group *Wilbertopora* species not only for the shape of its avicularia, but also for its combination of relatively small ordinary autozooids with large avicularia.

WILBERTOPORA IMPROCERA new species
Figure 12

Diagnosis.—Both avicularia and ordinary autozooids averaging under 0.5 mm long; avicularia otherwise resembling those of *W. spatulifera* n. sp., but with distal margins somewhat less flared.

Description.—Colonies start with an ancestrula, about 45%–50% as large as zooids in zones of repetition, that gives rise to a single zooid emanating from distal pore chamber; succeeding zooids arise from distal and one or both distolateral pore chambers, increasing in size gradually for two or three generations. Zooidal basal walls calcified. Ordinary autozooids rounded hexagonal to elliptical, averaging slightly less than 0.5 mm long and slightly more than 0.25 mm wide, widest near midlength; gymnocyst smooth, slightly convex except in zooids on which ovicells are developed, slightly broader proximally than laterally; mural rim prominent but rounded, enclosing an oval to elliptical aperture that occupies the distal 80%–85% of zooid length and the medial 80% of zooid width; cryptocyst a crescent-shaped ledge, slightly broader proximally than laterally, sloping inward, with a finely pustulose surface; opesia similar in shape to aperture, occupying approximately 90% of aperture length and 80% of aperture width; two oral spines present in few zooids. Avicularia approximately same length as ordinary autozooids, but about 25% narrower; gymnocyst smooth, strongly inflected laterally, but not forming distinct condyles; cryptocyst a narrow ledge at proximal margin of aperture; distal portion slightly more than 50% of total aperture length and 80%–85% of total aperture width; distal rim slightly more elevated than that of ordinary autozooid, moderately flared into spatulate shape, with a gently sloping distal shelf extending nearly halfway to gymnocystal inflections to form mandibular palate. Ovicells formed on proximal portion of gymnocyst of zooid distal to maternal zooid, which is an ordinary autozooid; rarely, ovicell can occur on zooid distal to avicularium, whose distal margin apparently occludes ovicell opening; gymnocyst of ovicell-bearing zooid slightly concave to serve as floor of brood

chamber; ovicell surface similar to that of gymnocyst, with a faint median suture; ovicell opening arcuate.

Etymology.—Latin, *improcerus*, short, low of stature, in allusion to the lengths of its autozooids and avicularia.

Types.—Holotype USNM 216163, HTL-23; paratype USNM 526325, HTL-14; paratype USNM 526326, HTL-33; paratype USNM 526327, HTL-43; paratypes USNM 216151, USNM 216152, USNM 526328, HTL-48; paratype USNM 526329, HTL-96; paratypes NHM BZ1311, NHM BZ1312.

Measurements.—See Table 4.

Other material examined.—USNM 216161, USNM 526330, USNM 526331, HTL-25; USNM 526332, USNM 526333, HTL-96; USNM 526334, HTL-173; USNM 526335, HTL-201; USNM 526336, HTL-225.

Occurrence.—Upper Albian, Fort Worth Formation, Love and Choctaw counties, Oklahoma, Cooke and Denton counties, Texas; Denton Formation, Grayson, Tarrant, and Johnson counties, Texas. Lower Cenomanian, Georgetown Formation, Williamson County, Texas.

Discussion.—Ovicells in *W. improcera* are in some cases positioned distal to avicularia, as in *W. listokinae* n. sp., but also seemingly were nonfunctional because the ovicell opening is then blocked by the raised distal margin of the avicularium.

WILBERTOPORA ACUMINATA new species
Figure 13

Wilbertopora sp. BOARDMAN AND CHEETHAM, 1973, fig. 40, b.
Wilbertopora mutabilis; CHEETHAM, 1975, pl. 3, fig. 4; CHEETHAM AND COOK, 1983, fig. 81.1.

Diagnosis.—Both avicularia and ordinary autozooids averaging well under 0.5 mm long; avicularia much narrower than autozooids, with distal portion of avicularian aperture narrowed to a point.

Description.—Colonies start with an ancestrula, about 50% as large as zooids in zones of repetition, that gives rise to a single zooid emanating from distal pore chamber; succeeding zooids arise from distal and one or both distolateral pore chambers, increasing in size gradually for two generations. Zooidal basal walls calcified. Autozooids rounded hexagonal to elliptical, averaging slightly more than 0.4 mm long and about 0.25 mm wide, widest near midlength; gymnocyst smooth, slightly convex except in zooids on which ovicells are developed, moderately broader proximally than laterally; mural rim prominent but rounded, enclosing an oval to elliptical aperture that occupies the distal 75%–80% of zooid length and the medial 85% of zooid width; cryptocyst a crescent-shaped ledge, slightly broader proximally than laterally, sloping inward, with a finely pustulose surface; opesia similar in shape to aperture, occupying approximately 85%–90% of aperture length and 80% of aperture width; two oral spines and, less commonly, an additional lateral spine present on some zooids. Avicularia approximately same length as autozooids, but about 40% narrower; gymnocyst smooth, broader both proximally and laterally than that of autozooids, forming distinct, blunt condyles for mandible; cryptocyst a narrow, crescent-shaped ledge at proximal margin of aperture; distal portion slightly more than 50% of total aperture length and about 40% of total aperture width; distal rim distinctly more elevated than that of autozooid, projecting slightly to moderately beyond proximal margin of distal zooid forming a narrow, pointed rostrum with narrow shelf extending nearly to condyles to form mandibular palate. Ovicells formed on proximal portion of gymnocyst of zooid distal to maternal zooid, which is an autozooid; ovicell-bearing zooid either an autozooid or an avicularium; gymnocyst of ovicell-bearing zooid slightly concave to serve as floor of brood chamber; ovicell surface similar to that of gymnocyst, with a faint median suture; ovicell opening arcuate.

Etymology.—Latin, *acuminatus*, pointed, sharpened, in allusion to the shape of the distal portion of the avicularium.

Types.—Holotype USNM 216143, HTL-89; paratype USNM 186571, HTL-94; paratype USNM 526337, HTL-36; paratype USNM 526338, HTL-37; paratypes NHM BZ1479, NHM BZ2295.

Measurements.—See Table 4.

Other material examined.—USNM 526339, HTL-36; USNM 526340, HTL-37.

Occurrence.—Lower Cenomanian, Main Street Formation, Tarrant County, Texas; Grayson Formation, Bryan County, Oklahoma, Grayson, Denton, Tarrant, Johnson, McLennan, Bell, and Travis counties, Texas.

Discussion.—*W. acuminata* stands out among the Washita Group *Wilbertopora* species because of its pointed avicularia. In this, it resembles *W. woodwardi* (Brydone) from the British Chalk (Turonian–Campanian), although avicularia in the latter species have complete cross bars (Taylor, 2002, pl. 9, fig. 2).

WILBERTOPORA HOADLEYAE new species
Figure 14

Diagnosis.—Avicularia slightly more than half the size of autozooids, with broadly rounded distal margin and distinct, rounded mandibular condyles.

Description.—Colonies start with an ancestrula, about 45%–50% as large as zooids in zones of repetition, that gives rise to a single zooid emanating from distal pore chamber; succeeding zooids arise from distal and one or both distolateral pore chambers, increasing in size gradually for two or three generations. Zooidal basal walls calcified. Autozooids rounded hexagonal to elliptical, averaging about 0.5 mm long and 0.3 mm wide, widest at or proximal to midlength; gymnocyst smooth, slightly convex except in zooids on which ovicells are developed, slightly broader proximally than laterally; mural rim prominent but rounded, enclosing an oval to elliptical aperture that occupies the distal 75%–80% of zooid length and the medial 80%–85% of zooid width; cryptocyst a crescent-shaped ledge, slightly broader proximally than laterally, sloping inward, with a finely pustulose surface; opesia similar in shape to aperture, occupying approximately 85% of aperture length and width; oral spines not seen. Avicularia about 55%–60% as long and 50%–55% as wide as autozooids, roughly rhombic in shape; gymnocyst smooth, broadest distally where it forms an elevated, hoodlike distal border for the avicularian aperture; cryptocyst a narrow ledge at proximal margin of aperture; distal portion slightly less than 50% of total aperture length and 75% of total aperture width; distal rim slightly more elevated than that of ordinary autozooid, broadly rounded, with a gently sloping distal shelf forming mandibular palate. Ovicells formed on proximal portion of gymnocyst of zooid distal to maternal zooid, which is an ordinary autozooid; gymnocyst of ovicell-bearing zooid slightly concave to serve as floor of brood chamber; ovicell surface similar to that of gymnocyst, with a faint median suture; ovicell opening arcuate.

Etymology.—Named for Carol Hoadley.

Types.—Holotype USNM 526341, paratype USNM 526342, HTL-9; paratypes USNM 526343, USNM 526344, HTL-48; paratype NHM BZ1326.

Measurements.—See Table 4.

Other material examined.—USNM 526345, USNM 526346, HTL-9; USNM 526347, HTL-14.

Occurrence.—Upper Albian, Fort Worth Formation, Cooke, Grayson, and Denton counties, Texas.

Discussion.—Although the distinctive avicularia of this species, the smallest in the Washita Group *Wilbertopora* species, appear

to represent one of the most advanced stages of avicularian differentiation (along with those of *W. acuminata* n. sp.), *W. hoadleyae* occurs much lower in the section than at least one species, *W. listokinae* n. sp., with much less differentiated avicularia.

ACKNOWLEDGMENTS

This work was supported by the Marie Bohrn Abbott Fund of the National Museum of Natural History (AHC and JS), and by a postdoctoral fellowship to ANO from the Alexander von Humboldt Foundation and a grant from the European Community, SYS-Resource Fund. NHM volunteer R. Prebble helped to curate material. We thank S. Hageman and R. L. Anstey for reviewing the manuscript.

REFERENCES

BANTA, W. C. 1973. Evolution of avicularia in cheilostome Bryozoa, p. 295–303. *In* R. S. Boardman, A. H. Cheetham, and W. A. Oliver Jr. (eds.), Animal Colonies: Development and Function through Time. Dowden, Hutchinson, and Ross, Stroudsburg, Pennsylvania.

BANTA, W. C. 1975. Origin and early evolution of cheilostome Bryozoa, p. 565–582. *In* Simone Pouyet (ed.), Bryozoa 1974. Documents des Laboratoires de Géologie de la Faculté des Sciences de Lyon, hors-série 3, fasc. 2.

BOARDMAN, R. S., AND A. H. CHEETHAM. 1969. Skeletal growth, intracolony variation, and evolution in Bryozoa: A review. Journal of Paleontology, 43:205–233.

BOARDMAN, R. S., AND A. H. CHEETHAM. 1973. Degrees of colony dominance in stenolaemate and gymnolaemate Bryozoa, p. 121–220. *In* R. S. Boardman, A. H. Cheetham, and W. A. Oliver Jr. (eds.), Animal Colonies: Development and Function through Time. Dowden, Hutchinson, and Ross, Stroudsburg, Pennsylvania.

BRYDONE, R. M. 1910. Notes on new or imperfectly known Chalk Polyzoa. Geological Magazine, Decade 5, 7:258–260.

BUDD, A. F., AND A. G. COATES. 1992. Nonprogressive evolution in a clade of Cretaceous *Montastraea*-like corals. Paleobiology, 18:425–446.

CANU, F. 1900. Révision des Bryozoaires du Crétacé figurés par d'Orbigny. Deuzièm partie—Cheilostomata. Bulletin de la Société Géologique de France, série 3, 28:334–463.

CHEETHAM, A. H. 1954. A new Early Cretaceous bryozoan from Texas. Journal of Paleontology, 28:177–184.

CHEETHAM, A. H. 1975. Taxonomic significance of autozooid size and shape in some early multiserial cheilostomes from the Gulf Coast of the U. S. A., p. 547–564. *In* Simone Pouyet (ed.), Bryozoa 1974. Documents des Laboratoires de Géologie de la Faculté des Sciences de Lyon, hors-série 3, fasc. 2.

CHEETHAM, A. H. 1986. Tempo of evolution in a Neogene bryozoan: Rates of morphologic change within and across species boundaries. Paleobiology, 12:190–202.

CHEETHAM, A. H., AND P. L. COOK. 1983. General features of the class Gymnolaemata, p. 138–207. *In* R. A. Robison (ed.), Treatise on Invertebrate Paleontology. Pt. G. Bryozoa. Geological Society of America and University of Kansas Press, Lawrence.

CHEETHAM, A. H., AND D. M. LORENZ. 1976. A vector approach to size and shape comparisons among zooids in cheilostome bryozoans. Smithsonian Contributions to Paleobiology, Number 29, 55 p.

CHEETHAM, A. H., J. B. C. JACKSON, AND J. SANNER. 2001. Evolutionary significance of sexual and asexual modes of propagation in Neogene species of the bryozoan *Metrarabdotos* in tropical America. Journal of Paleontology, 75:564–577.

COOK, P. L. 1968. Polyzoa from West Africa, the Malacostega, Pt. I. Bulletin of the British Museum (Natural History), Zoology, 16(3):115–160.

COOK, P. L. 1979. Some problems in interpretation of heteromorphy and colony integration in Bryozoa, p. 193–210. *In* G. P. Larwood and B. R. Rosen (eds.), Biology and Systematics of Colonial Organisms. Academic Press, London.

CUFFEY, R. J., R. M. FELDMAN, AND K. E. POHLABLE. 1981. New Bryozoa from the Fox Hills Sandstone (Upper Cretaceous, Maestrichtian) of North Dakota. Journal of Paleontology, 55:401–409.

DZIK, J. 1975. The origin and early phylogeny of the cheilostomatous Bryozoa. Acta Palaeontologica Polonica, 20:395–423.

FARRIS, J. S. 1988. Hennig 86 Reference, Version 1.5. Farris, Stony Brook, New York, 17 p.

GORDON, D. P. 1984. The marine fauna of New Zealand, Bryozoa: Gymnolaemata from the Kermadec Ridge. New Zealand Oceanographic Institute, Memoir 91, 198 p.

GRAY, J. E. 1848. List of the Specimens of British Animals in the Collection of the British Museum. Pt. 1. Centroniae or Radiated Animals. British Museum, London, 173 p.

GUHA, A. K. 1989. Upper Cretaceous cheilostomes (Bryozoa) from the Bagh sediments of Madhya Pradesh, p. 118–131. *In* P. Kalia (ed.), Micropaleontology of the Shelf Sequences of India. Papyrus Publishing House, New Delhi.

HERRERA-CUBILLA, A., M. H. DICK, J. SANNER, AND J. B. C. JACKSON. In press. Neogene Cupuladriidae of tropical America, I, Taxonomy of Recent *Cupuladria* from opposite sides of the Isthmus of Panama. Journal of Paleontology, 80(2).

JACKSON, J. B. C., AND A. H. CHEETHAM. 1990. Evolutionary significance of morphospecies: A test with cheilostome Bryozoa. Science, 248:579–583.

JACKSON, J. B. C., AND A. H. CHEETHAM. 1994. Phylogeny reconstruction and the tempo of speciation in cheilostome Bryozoa. Paleobiology, 20:407–423.

LANG, W. D. 1915. On some new uniserial Cretaceous cheilostome Polyzoa. Geological Magazine, decade 6, 2:496–504.

MARCUS, E. 1938. Bryozoarios marinhos Brasileiros, II. Boletins da Faculdade de Philosofia, Sciencias e Letras, IV, Zoologia, 2:1–196.

NORMAN, A. M. 1903. Notes on the natural history of East Finmark, Polyzoa. Annals and Magazine of Natural History, Series 7, 11:567–598.

NORUSIS, M. J. 1994a. SPSS Base System, 6.1. SPSS, Inc., Chicago, 941 p.

NORUSIS, M. J. 1994b. SPSS Professional Statistics, 6.1. SPSS, Inc., Chicago, 385 p.

OSTROVSKY, A. N., AND P. D. TAYLOR. In press. Early stages of the ovicell development in the calloporid *Wilbertopora* (Bryozoa: Cheilostomata) from the Upper Cretaceous of the USA. Proceedings of the 13th IBA Conference, Concepcion, Chile.

PAGE, R. D. M. 1996. Treeview, an application to display phylogenetic trees on personal computers. Computer Applications in the Biosciences, 12:357–358.

POHOWSKY, R. A. 1973. A Jurassic cheilostome from England, p. 447–461. *In* G. P. Larwood (ed.), Living and Fossil Bryozoa. Academic Press, London.

RYLAND, J. S., AND D. P. GORDON. 1977. Some New Zealand and British species of *Hippothoa* (Bryozoa: Cheilostomata). Journal of the Royal Society of New Zealand, 7:17–49.

SILÉN, L. 1945. The main features of the development of the ovum, embryo and ooecium in the ooeciferous Bryozoa Gymnolaemata. Arkiv för Zoologi, 35A(17):1–34.

SWOFFORD, D. L. 2000. PAUP*, phylogenetic analysis using parsimony (*and other methods), version 4. Sinauer Associates, Sunderland, Massachusetts.

TAYLOR, P. D. 1986. *Charixa* Lang and *Spinicharixa* gen. nov., cheilostome bryozoans from the Lower Cretaceous. Bulletin of the British Museum (Natural History), Geology Series, 40:197–222.

TAYLOR, P. D. 1988. Major radiation of cheilostome bryozoans: Triggered by the evolution of a new larval type? Historical Biology, 1:45–64.

TAYLOR, P. D. 1994. An early cheilostome bryozoan from the Upper Jurassic of Yemen. Neues Jahrbuch für Geologie und Paläontologie Abhandlungen, 191:331–344.

TAYLOR, P. D. 2002. Bryozoans, p. 53–75. *In* A. B. Smith and D. J. Batten (eds.), Fossils of the Chalk (second edition). Palaeontological Association, London.

TAYLOR, P. D., AND R. M. BADVE. 1994. The mid-Cretaceous bryozoan fauna from the Bagh Beds of central India: Composition and evolutionary significance, p. 181–186. *In* P. J. Hayward, J. S. Ryland, and P. D. Taylor (eds.), Biology and Palaeobiology of Bryozoans. Olsen and Olsen, Fredensborg.

WINSTON, J. E. 1984. Why bryozoans have avicularia—A review of the evidence. American Museum Novitates, 2789:1–26.

WINSTON, J. E. 1986. Victims of avicularia. Marine Ecology, 7:193–199.

WINSTON, J. E. 1991. Avicularian behavior—A progress report, p. 531–

540. *In* Françoise P. Bigey (ed.), Bryozoaires Actuels et Fossiles: Bryozoa Living and Fossil. Bulletin de la Société des Sciences Naturelles de l'Ouest de la France, Mémoire Hors Série, 1.

ACCEPTED 7 DECEMBER 2004

APPENDIX 1

Register of localities

Material in the Department of Paleobiology, National Museum of Natural History, Smithsonian Institution, Washington, DC (NMNH), collected by A. Loeblich Jr. and H. T. Loeblich, is from the following localities:

HTL-1, Grayson Formation, at Grayson Bluff, a high, southwest-facing bluff on Denton Creek, 3.5 mi northeast of Roanoke, 2 mi by road east of the Fort Worth-Denton highway, Denton County, Texas.

HTL-5, Grayson Formation, in a road cut and the creek bank of a tributary to Little Mineral Creek, 50 ft west of the road and north of the road cut, about 0.88 mi south of Fink (locally called Georgetown) and 2.5 mi north of Pottsboro, northwestern Grayson County, Texas.

HTL-8, Grayson Formation, 3.0–5.5 ft above the Main Street limestone in a road cut on the south bank of Chuckwa Creek, on the west side of U.S. Highway 75, one mile north of Durant, in the NE1/4, sec. 29, T6S, R9E, Bryan County, Oklahoma.

HTL-9, Fort Worth Formation, in a deep road cut on the west side of Highway 75, Denison-Durant highway, 1,000 ft north of Calvary Cemetery, 0.5 mi north of the Texas Highway Department Information station, 1.6 mi north of Main Street in Denison, Grayson County, Texas.

HTL-11, Georgetown Formation, 3 ft below the top of the Georgetown Formation, in the bank of Shoal Creek, opposite Twenty-Second Street in Austin, Travis County, Texas.

HTL-14, Fort Worth Formation, exposure in two low road cuts near the bend of the road in the northeast corner of sec. 28, T8S, R2E, on the east side of the road in Love County, Oklahoma.

HTL-25, Denton Formation, in the creek bank in Munson Park, west of Highway 75 and just north of exit from park, 1.1 mi north of Main Street in Denison, Grayson County, Texas.

HTL-31, Grayson Formation, along the hillside and in the banks of a small creek, at the proposed road of Fifth Avenue, between Nelson and Sheppard streets, in the southwest part of the city of Denison, Grayson County, Texas.

HTL-33, Denton Formation, on Armstrong Avenue, 0.5 mi north of the city standpipe in Denison, Grayson County, Texas.

HTL-36, Main Street Formation, in a road cut, on the road leading eastward to Grayson Bluff from the Fort Worth-Denton highway, about one mile east of the highway, 3.5 mi northeast of Roanoke, Denton County, Texas.

HTL-37, Main Street Formation, in deep road cut on Denton-Aubrey road, about 0.1 mi south of the bridge over Clear Creek, 4.8 mi by road northeast of Denton County courthouse square in Denton, Denton County, Texas.

HTL-39, Fort Worth Formation, creek bank just north of the small concrete bridge where the road crosses a tributary of Hickory Creek, 1.25 mi northwest of Krum, Denton County, Texas.

HTL-41, Fort Worth Formation, on the southwest corner of intersection of West Berry and Merida streets, at small east-facing cliff that was the west bank of a small creek, 0.7 mi east of the southeast corner of Texas Christian University campus, Fort Worth, Tarrant County, Texas.

HTL-43, Fort Worth Formation, 100 yds east of underpass under Frisco Railroad, in the banks of a small stream, on the Frisco Road, which branches from the Old Cleburne Road, crossing the Frisco tracks 0.3 mi south of Berry Street in Fort Worth, Tarrant County, Texas.

HTL-45, Main Street Formation, in a railroad cut of the Santa Fe Railroad, 200 ft south of a point where the road to the seminary from the west crosses the tracks, about 300 ft west of the Baptist Seminary Campus, southwest of Fort Worth, Tarrant County, Texas.

HTL-47, Denton Formation, on the south bank of a tributary of Sycamore Creek, which was dammed to form Katy Lake, 0.25 mi east of and below the Katy Lake Dam, southeast of Fort Worth, Tarrant County, Texas.

HTL-48, Fort Worth Formation, road cut on the east side of U.S. Highway 77, one mile west-southwest of the Gainesville courthouse square, just south of a small bridge in Cooke County, Texas.

HTL-53, Fort Worth Formation, exposure a low 10-ft, north-facing cliff forming the south bank of the south branch of Noland's River. A road leaving the Godley-Cresson highway turns directly south and leads to within 250 ft of the exposure where it turns westward, about 0.5 mi southwest of Godley, Johnson County, Texas.

HTL-54, Denton Formation, exposure along the steep west bank of the north fork of Noland's River, about 100 ft south of bridge on the Godley-Joshua road, 1.4 mi northeast of Godley, Johnson County, Texas.

HTL-55, Paw Paw Formation, in road cut on the south side of the road, at the western edge of the Federal Narcotic Farm, southeast of Fort Worth, Tarrant County, Texas.

HTL-56, Fort Worth Formation, road cut in the 1,700 block of East Lancaster Street, just west of the corner of Riverside Drive and Lancaster Street, on the Fort Worth-Dallas highway (Highway 80) in eastern Fort Worth, Tarrant County, Texas.

HTL-67, Fort Worth Formation, in a west-facing creek bank, just north of U.S. Highway 70, and across the railroad tracks, in the southwest quarter of the NE1/4, sec. 20, T6S, R7E, about 0.9 mi east of Aylesworth, Marshall County, Oklahoma.

HTL-81, Denton Formation, in the Gainesville Brick Pit, an unworked pit southeast of Gainesville, Cook County, Texas.

HTL-85, Fort Worth Formation, on the north bank of a small stream, east of the road, in the middle of the 2,900 block of Frazier Street in Fort Worth, Tarrant County, Texas.

HTL-86, Main Street Formation, in the west-facing cliff of a small stream east of the road, 3.9 mi south of the southeast edge of the Baptist Seminary campus, on the road leading south, one block east of the eastern edge of the campus (the Fort Worth-Crowley Road), south of Fort Worth, Tarrant County, Texas.

HTL-87, Grayson Formation, exposure of Village Creek, where the stream bends about 100 yds south of the bridge on the Everman-Kennedale Road, two miles east of Everman, southeast of Fort Worth, Tarrant County, Texas.

HTL-89, Grayson Formation, in the east bank of a small tributary to Salado Creek, just north of a small fault, about 400 yds east of Highway 81, 2.4 mi south of the bridge across Salado Creek in Salado, Bell County, Texas.

HTL-90, Grayson Formation (Del Rio Shale), at the base of the exposure on the west bank of Shoal Creek, just south of the bridge on Thirty-Fourth Street, and just north of a fault in Austin, Travis County, Texas.

HTL-94, Grayson Formation, exposure in the bank of Barton Creek where the Barton Springs Road crosses the creek southwest of Austin, Travis County, Texas.

HTL-96, Georgetown Formation, along Smith Branch, the first main creek east of Georgetown, from one mile north of the highway, upstream to Highway 104, Williamson County, Texas.

HTL-97, Main Street Formation, just east of the railroad underpass under the Santa Fe Railroad, on the Belton-Temple highway, U.S. Highway 81, northeast of Belton, Bell County, Texas.

HTL-99, Denton Formation, in roadside ditch on east side of road leading south from Rio Vista, on the northeast corner where a less-traveled east branch road turns from the main south road, one mile south of the garage and filling station near the eastern edge of the town of Rio Vista, in southern Johnson County, Texas.

HTL-101, Main Street Formation, at an underpass under the Santa Fe Railroad, just south of Cleburne, on the Cleburne-Hillsboro Road, Johnson County, Texas.

HTL-103, Grayson Formation, a steep northwest-facing slope, 0.75 mi due east of Burleson, 0.2 mi northeast of the old Burleson-Alvarado Road in Johnson County, Texas.

HTL-170, Kiamichi Formation, in a deep road cut on Stove Foundry Road, just north of the new Texas and Pacific Railroad shops, Fort Worth, Tarrant County, Texas.

HTL-173, Fort Worth Formation, 3.5 mi north of the Ponder railroad station, in road cut east of the road, just north of the bridge over South Hickory Creek, on the Ponder-Krum Road, Denton County, Texas.

HTL-201, Fort Worth Formation, in a road cut on the north side of the road, 0.4 mi northeast of Denton Creek, 1.6 mi east of the Justin-Ponder Road in Justin, Denton County, Texas.

HTL-225, Fort Worth Formation, in a road cut on the east side of the road, 0.6 mi south of the northwest corner of sec. 1, T7S, R19E, Choctaw County, Oklahoma.

Material in NMNH collected by N. E. Nelson is from the following locality:

USNM 526291, USNM 526318, Paw Paw Formation, on old Everman Road, 6.5 mi south of Fort Worth, Tarrant County, Texas.

Material in the Department of Palaeontology, the Natural History Museum, London (NHM) collected by M. Listokin, C. Hoadley, or A. Smith and P. Taylor is from the following localities:

NHM BZ1123-BZ1125, Weno Formation, B6, stream cuts 3 mi north of Bokchito, and road cuts 4.1 mi north of Bokchito, Bryan County, Oklahoma.
NMH BZ1311, BZ1312, B2, Denton Formation, stream cuts east of gravel road, 0.5 mi south of Cobb, Bryan County, Oklahoma.
NHM BZ1326, same as HTL-9.
NHM BZ1372, Main Street Formation, in bluish gray clay off Crowley Road, southern Fort Worth, Tarrant County, Texas.
NHM BZ1479, same as HTL-11.
NHM BZ1614, BZ1352, BZ1627, Grayson Formation, Mancini 6, Section on southeast face of the Lake Waco Dam spillway cut, at 150 yds (Units A and B); and at 250 yds (Unit C-1), east of the Lake Waco Dam Spillway, Waco, McLennan County, Texas.
NHM BZ1699, BZ1700, same as HTL-1.
NHM BZ1856, BZ1912, D58502, D58503, Grayson Formation, Waco Dam Borrow Pit, Waco, McLennan County, Texas.
NHM BZ2275, Georgetown Formation, Bosque River, south of Evergreen Cemetery, near McGregor Municipal Airport, McLennan County, Texas.
NHM BZ2295, Grayson Formation, overgrown bank at end of minor road south of, and parallel to, Farm Road 1171, Lake Grapevine, Denton County, Texas.
NHM D47068, same as HTL-39.
NHM D57378, Grayson Formation, Del Rio Shale Pit, behind Lake Waco Dam, McLennan County, Texas.
NHM D58508–58510, PEI 49, Grayson Formation, west face of hill, south of Lake Waco, near Old Dettay's Crossing, 2 mi north of Speegleville, McLennan County, Texas.

Material in the H. V. Howe Collection, Department of Geology and Geophysics, Louisiana State University, Baton Rouge (LSU), collected by J. W. West and W. F. Roux, is from the following locality:

Fort Worth Formation, at a highway bridge over a tributary of Hickory Creek, 1.25 mi northwest of Krum, Denton County, Texas.

APPENDIX 2

Characters used in discriminant analysis of *Wilbertopora* species

The full set of 60 morphological characters listed below was employed in distinguishing Washita Group species of *Wilbertopora* using a series of canonical discriminant analyses (DA), as described in the text. Each of the subset of 18 characters in capital letters was significant (at $P < 0.05$) in the final discriminant analysis (i.e., remained in the analysis after 18 steps after which the discriminating ability of the procedure was exhausted); the character's rank in the final analysis is given in parentheses following the character name; ranges are for means of the colony means within species.

Ordinary autozooids (Fig. 2.1)

1. *Zooid length.*—Distalmost point on outer edge of mural rim to corresponding point on next proximal zooid; range, 0.4083–0.5509 mm.
2. *Zooid width.*—Maximum distance between outer lateral margins of gymnocyst; range, 0.2455–0.3147 mm.
3. *Aperture length.*—Distalmost point on crest of mural rim to its proximalmost point (presumably corresponding to the combined operculum-frontal membrane length); range, 0.3058–0.4321 mm.
4. *Aperture width.*—Maximum distance between lateral crests of mural rim (presumably corresponding to frontal membrane width); range, 0.2037–0.2614 mm.
5. *Opesia length (11).*—Distalmost point on crest of mural rim to proximalmost point on inner margin of cryptocyst; range, 0.2615–0.3857 mm.
6. *Opesia width.*—Maximum distance between inner lateral margins of cryptocyst; range, 0.1597–0.2209 mm.

Avicularia (Fig. 2.2)

7. *Zooid length (4).*—Measured as in character 1; range, 0.2740–0.5956 mm.
8. *Zooid width (6).*—Measured as in character 2; range, 0.1539–0.3169 mm.
9. *Proximal aperture length (9).*—Distance between a line connecting inward inflections of lateral mural rim and proximalmost point on mural rim (presumably corresponding to frontal membrane length); range, 0.0928–0.3091 mm.
10. *Proximal aperture width (15).*—Measured as in character 4; range, 0.0802–0.2361 mm.
11. *Distal aperture length (5).*—Distance between distalmost point on crest of mural rim and a line connecting inward inflections of lateral mural rim (presumably corresponding to mandible length); range, 0.0819–0.3077 mm.
12. *Distal aperture width (1).*—Maximum distance between lateral crests of mural rim in portion of aperture distal to line connecting inward inflections (presumably corresponding to mandible width); range, 0.0440–0.1979 mm.

Maternal autozooids (Fig. 2.3)

13. *Zooid length.*—Not shown; measured as in character 1; range, 0.3683–0.5196 mm.
14. *Zooid width.*—Not shown; measured as in character 2; range, 0.2461–0.3088 mm.
15. *Aperture length.*—Not shown; measured as in character 3; range, 0.2787–0.4136 mm.
16. *Aperture width (10).*—Not shown; measured as in character 4; range, 0.1820–0.2501 mm.
17. *Opesia length.*—Not shown; measured as in character 5; range, 0.2343–0.3683 mm.
18. *Opesia width.*—Not shown; measured as in character 6; range, 0.1478–0.2051 mm.

Zooids distal to maternal zooids (Fig. 2.3)

19. *Ovicell length.*—Distalmost margin of ovicell to proximal ''horns'' overlapping distal margin of maternal zooid (note that, because of the shape of the ovicell opening, the overlap does not obscure the distalmost point on the maternal zooid's mural rim); range, 0.1402–0.1839 mm.
20. *Ovicell width.*—Maximum distance between lateral margins of ovicell; range, 0.1502–0.1833 mm.
21. *Zooid length.*—Not shown; measured as in character 1; range, 0.3760–0.5329 mm.
22. *Zooid width.*—Not shown; measured as in character 2; range, 0.2432–0.3275 mm.
23. *Aperture length.*—Not shown; measured as in character 3; range, 0.2710–0.4158 mm.
24. *Aperture width.*—Not shown; measured as in character 4; range, 0.1980–0.2795 mm.
25. *Opesia length (13).*—Not shown; measured as in character 5; range, 0.2378–0.3646 mm.
26. *Opesia width.*—Not shown; measured as in character 6; range, 0.1478–0.2255 mm.

Ratios (''shape'' characters)

27. *Length/width, ordinary autozooids.*—Character 1/character 2, relative zooidal elongation; range, 1.4266–1.9255.
28. *Aperture length/aperture width, ordinary autozooids.*—Character 3/character 4, relative apertural elongation; range, 1.4288–1.8330.
29. *Aperture length/zooid length, ordinary autozooids (7).*—Character 3/character 1, proportion of zooid length occupied by frontal membrane-operculum complex (also an indirect measure of the extent of the proximal gymnocyst); range, 0.7250–0.8647.
30. *Aperture width/zooid width, ordinary autozooids.*—Character 4/character 2, proportion of zooid width occupied by frontal membrane; range, 0.7216–0.8787.
31. *Opesia length/aperture length, ordinary autozooids.*—Character 5/character 3, proportion of aperture length occupied by opesia, the inverse of the proportion occupied by the cryptocyst; range, 0.8500–0.9134.
32. *Opesia length/opesia width, ordinary autozooids.*—Character 5/character 6, relative elongation of opesia; range, 1.5866–2.0785.
33. *Opesia width/aperture width, ordinary autozooids.*—Character 6/

character 4, proportion of aperture width occupied by opesia, the inverse of the proportion occupied by the cryptocyst; range, 0.7455–0.8483.

34. *Avicularium length/avicularium width.*—Character 7/character 8, relative elongation of avicularium; range, 1.4291–2.7675.
35. *Avicularium length/autozooid length (8).*—Character 7/character 1, relative length of avicularium compared to ordinary autozooids; range, 0.5496–1.2407.
36. *Avicularium width/autozooid width.*—Character 8/character 2, relative width of avicularium compared to ordinary autozooids; range, 0.5562–1.0494.
37. *Proximal aperture length/proximal aperture width, avicularium (16).*—Character 9/character 10, relative elongation of proximal aperture; range, 0.8349–1.4747.
38. *Distal aperture length/distal aperture width, avicularium (3).*—Character 11/character 12, relative elongation of distal aperture (''shape'' of mandible); range, 0.7159–3.6388.
39. *Distal aperture length/avicularium length (2).*—Character 11/character 7, proportion of avicularium occupied by mandible; range, 0.1872–0.5161.
40. *Avicularium distal aperture length/autozooid opesia length.*—Character 11/character 5, proportion of length of autozooidal frontal membrane-operculum complex equivalent to length of avicularian mandible; range, 0.2251–0.8533.
41. *Avicularium distal aperture width/autozooid opesia width (14).*—Character 12/character 6, proportion of width of autozooidal frontal-membrane-operculum complex equivalent to width of avicularian mandible; range, 0.2587–1.1022.
42. *Maternal zooid length/maternal zooid width.*—Character 13/character 14, relative zooidal elongation; range, 1.4563–1.7637.
43. *Maternal zooid length/ordinary autozooid length (18).*—Character 13/character 1, relative length of maternal zooid compared to ordinary autozooid; range, 0.9138–0.9788.
44. *Maternal zooid width/ordinary autozooid width.*—Character 14/character 2, relative width of maternal zooid compared to ordinary autozooid; range, 0.8831–1.0147.
45. *Aperture length/aperture width, maternal zooid.*—Character 15/character 16, relative apertural elongation; range, 1.3951–1.8901.
46. *Aperture length/zooid length, maternal zooid.*—Character 15/character 13, proportion of zooid length occupied by frontal membrane-operculum complex; range, 0.7569–0.8571.
47. *Aperture width/zooid width, maternal zooid.*—Character 16/character 14, proportion of zooid width occupied by frontal membrane; range, 0.7576–0.8656.
48. *Opesia length/opesia width, maternal zooid.*—Character 17/character 18, relative elongation of opesia; range, 1.4951–2.0173.
49. *Opesia length/aperture length, maternal zooid.*—Character 17/character 15, proportion of aperture length occupied by opesia, the inverse of the proportion occupied by the cryptocyst; range, 0.8407–0.9388.
50. *Opesia width/aperture width, maternal zooid.*—Character 18/character 16, proportion of aperture width occupied by opesia, the inverse of the proportion occupied by the cryptocyst; range, 0.7414–0.8655.
51. *Ovicell length/ovicell width.*—Character 19/character 20, ovicell shape; range, 0.8819–1.0131.
52. *Length/width, zooid distal to maternal zooid.*—Character 21/character 22, relative zooidal elongation; range, 1.4650–1.9021.
53. *Length zooid distal to maternal zooid/length ordinary autozooid (17).*—Character 21/character 1, relative zooid length compared to ordinary autozooid; range, 0.9203–1.0197.
54. *Width zooid distal to maternal zooid/width ordinary autozooid (12).*—Character 22/character 2, relative zooid width compared to ordinary autozooid; range, 0.8737–1.0321.
55. *Aperture length/aperture width, zooid distal to maternal zooid.*—Character 23/character 24, relative apertural elongation; range, 1.2578–1.7250.
56. *Aperture length/zooid length, zooid distal to maternal zooid.*—Character 23/character 21, proportion of zooid length occupied by frontal membrane-operculum complex; range, 0.7088–0.8339.
57. *Aperture width/ zooid width, zooid distal to maternal zooid.*—Character 24/character 22, proportion of zooid width occupied by frontal membrane-operculum complex; range, 0.7484–0.9024.
58. *Opesia length/opesia width, zooid distal to maternal zooid.*—Character 25/character 26, relative elongation of opesia; range, 1.4358–1.9249.
59. *Opesia length/aperture length, zooid distal to maternal zooid.*—Character 25/character 23, proportion of aperture length occupied by opesia, the inverse of the proportion occupied by the cryptocyst; range, 0.8416–0.9755.
60. *Opesia width/aperture width, zooid distal to maternal zooid.*—Character 26/character 24, proportion of aperture width occupied by opesia, the inverse of the proportion occupied by the cryptocyst; range, 0.7466–0.8416.

APPENDIX 3

Characters and character states used in cladistic analysis of Washita Group species of *Wilbertopora*

Each of the subset of 20 characters listed below furnished two or more non-overlapping ranges of values in Duncan's Multiple Range tests (DMRT) on the 60 characters in Appendix 2, and thus was coded for use in constructing the hypothesis of relationship shown in Figure 4. Character numbers, names, and definitions correspond to those in Appendix 2. F, P, and degrees of freedom (d. f.) are given in parentheses for each character from the single-classification ANOVA on which the DMRT was based. The one-digit codes for states in each character in this subset vary from a simple linear sequence (e.g., 0, 1, 2, 3) to a nonlinear series (e.g., 0, 1, 4, 6), depending on the relative continuity or discontinuity of species means as discussed in the text. Coded character states for each species follow in the matrix at the end of this list. Characters 35 and 59 proved to be uninformative with regard to parsimony.

Ordinary autozooids

5. *Opesia length (F = 4.7647, P = 0.0004, d. f. = 7, 49).*—Coded states: 0 = 0.2615, 1 = 0.2835, 2 = 0.3357–0.3857.

Avicularia

7. *Zooid length (F = 13.2756, P = 0.0000, d. f. = 7, 85).*—Coded states: 0 = 0.2740, 2 = 0.4220–0.4276, 3 = 0.4674, 4 = 0.5304, 5 = 0.5728–0.5956.
8. *Zooid width (F = 43.5531, P = 0.0000, d. f. = 7, 85).*—Coded states: 0 = 0.1539, 1 = 0.1716, 2 = 0.2024, 3 = 0.2218–0.2326, 5 = 0.3027–0.3169.
9. *Proximal aperture length (F = 12.0698, P = 0.0000, d. f. = 7, 80).*—Coded states: 0 = 0.0928, 1 = 0.1461, 2 = 0.1814–0.2384, 4 = 0.3091.
10. *Proximal aperture width (F = 60.7416, P = 0.0000, d. f. = 7, 75).*—Coded states: 0 = 0.0802, 2 = 0.1145–0.1503, 4 = 0.2173–0.2361.
11. *Distal aperture length (F = 29.9586, P = 0.0000, d. f. = 7, 82).*—Coded states: 0 = 0.0819–0.0988, 2 = 0.1599–0.1648, 3 = 0.0.2004, 4 = 0.0.2314, 5 = 0.2560, 7 = 0.3077.
12. *Distal aperture width (F = 69.5897, P = 0.0000, d. f. = 7, 83).*—Coded states: 0 = 0.0440, 2 = 0.0699, 4 = 0.0989–0.1064, 6 = 0.1379, 7 = 0.1576, 8 = 0.1726, 9 = 0.1979.

Maternal autozooids

14. *Zooid width (F = 6.6733, P = 0.0000, d. f. = 7, 71).*—Coded states: 0 = 0.2461–0.2595, 1 = 0.2849, 2 = 0.2940–0.3088.

Zooids distal to maternal zooids

22. *Zooid width (F = 11.2233, P = 0.0000, d. f. = 7, 64).*—Coded states: 0 = 0.2432–0.2555, 1 = 0.2810, 2 = 0.0.3074, 3 = 0.3184–0.3275.

Ratios (''shape'' characters)

29. *Aperture length/zooid length, ordinary autozooids (F = 5.1820, P = 0.0002, d. f. = 7, 52).*—Coded states: 0 = 0.7250–0.7854, 1 = 0.8223, 2 = 0.8395–0.8647.
34. *Avicularium length/avicularium width (F = 21.4911, P = 0.0000, d. f. = 7, 83).*—Coded states: 0 = 1.4291–1.8330, 2 = 2.3244, 3 = 2.5065, 4 = 2.7269–2.7675.
35. *Avicularium length/autozooid length (F = 13.2803, P = 0.0000, d. f. = 7, 74).*—Coded states: 0 = 0.5496, 2 = 0.9968–1.0674, 4 = 1.2407.
36. *Avicularium width/autozooid width (F = 23.3558, P = 0.0000, d. f.*

= 7, 74).—Coded states: 0 = 0.5562, 1 = 0.6455, 2 = 0.7466, 3 = 0.8022–0.8306, 5 = 0.9837–1.0494.

37. *Proximal aperture length/proximal aperture width, avicularium (F = 20.1622, P = 0.0000, d. f. = 7, 72).*—Coded states: 0 = 0.8349, 1 = 1.0138, 2 = 1.1243, 3 = 1.2758, 4 = 1.3949–1.4747.
38. *Distal aperture length/distal aperture width, avicularium (F = 45.6379, P = 0.0000, d. f. = 7, 82).*—Coded states: 0 = 0.7159–1.2303, 1 = 1.6606, 2 = 1.9281, 4 = 3.3335–3.6388.
39. *Distal aperture length/avicularium length (F = 31.5764, P = 0.0000, d. f. = 7, 82).*—Coded states: 0 = 0.1872, 2 = 0.2808, 4 = 0.3783–0.4444, 6 = 0.5161.
40. *Avicularium distal aperture length/autozooid opesia length (F = 18.7407, P = 0.0000, d. f. = 7, 48).*—Coded states: 0 = 0.2251–0.2718, 2 = 0.6091–0.7123, 4 = 0.8533.
41. *Avicularium distal aperture width/autozooid opesia width (F = 24.5633, P = 0.0000, d. f. = 7, 47).*—Coded states: 0 = 0.2587–0.3149, 2 = 0.6394–0.7942, 4 = 1.0782–1.1022.
49. *Opesia length/aperture length, maternal zooid (F = 4.5938, P = 0.0008, d. f. = 7, 53).*—Coded states: 0 = 0.8407, 1 = 0.8486, 2 = 0.8886–0.9388.
59. *Opesia length/aperture length, zooid distal to maternal zooid (F = 5.4906, P = 0.0005, d. f. = 7, 46).*—Coded states: 0 = 0.8416–0.0.8958, 2 = 0.9755.

	Characters																			
Species	5	7	8	9	10	11	12	14	22	29	34	35	36	37	38	39	40	41	49	59
W. mutabilis	2	4	5	4	4	0	6	2	3	0	0	2	5	4	0	0	0	2	2	0
W. listokinae	2	5	5	2	4	4	9	2	2	0	0	2	5	1	0	4	2	4	2	0
W. tappanae	0	2	5	2	4	2	8	0	0	0	0	2	5	0	0	4	2	4	0	0
W. spatulifera	2	5	3	2	2	5	7	1	1	2	3	2	3	4	1	4	2	2	2	0
W. attenuata	2	5	3	2	2	7	4	0	0	2	4	4	3	4	4	6	4	2	?	?
W. improcera	2	3	2	2	2	3	4	0	0	1	2	2	2	4	2	4	2	2	2	?
W. acuminata	1	2	0	1	2	2	0	0	0	0	4	2	1	3	4	4	2	0	1	0
W. hoadleyae	2	0	1	0	0	0	2	2	3	0	0	0	0	2	0	2	0	0	2	2